Waters at the Edge

Tracking Greenland's Ice-Marginal Lakes with SWOT Observations

Lilian Reichel

Master Thesis

TU Delft: Master of Applied Earth Sciences

TU Delft

Waters at the Edge

Tracking Greenland's Ice-Marginal Lakes with SWOT Observations

by

Lilian Reichel

to obtain the degree of Master of Science
at the Delft University of Technology,
to be defended publicly on Friday August 29, 2025 at 13:00.

Student number:	5999049	
Project duration:	February 10, 2025 – August 29, 2025	
Thesis committee:	Dr. ir. B. Wouters,	TU Delft, Supervisor
	Dr. ir. D. C. Slobbe,	TU Delft, Supervisor
	Dr. S. L. M. Lhermitte,	TU Delft, Assessment Committee

An electronic version of this thesis is available at http://repository.tudelft.nl/.
Cover photo belongs to ESA, Pixabay/A. Dassel [28].

TU Delft

Preface

This thesis is submitted in partial fulfilment of the requirements for the degree of Master of Science in Applied Earth Sciences at the Delft University of Technology, under the supervision of Dr. ir. Bert Wouters and Dr. ir. Cornelis Slobbe. The research presented herein was conducted between the 10th of February and the 29th of August 2025, within the Department of Geoscience and Remote Sensing.

I would like to express my sincere gratitude to my supervisors for their continuous guidance and support throughout the course of this research. Their insight and constructive feedback greatly contributed to the quality and direction of this work.

Additionally, I am grateful to my fellow AES students and friends, for their assistance, discussions, and moral support throughout the journey.

Last but not least, I would like to thank my family for their support and encouragement, without which this would not have been possible.

Lilian Reichel
Delft, August 2025

Abstract

The Surface Water and Ocean Topography (SWOT) mission has the goal to observe global lakes and reservoirs with a size as small as 1 ha and ocean circulations at sub-mesoscale with the help of the Ka-band Radar Interferometer (KaRIn) wide-swath altimeter. Launched in 2022, SWOT is observing an unprecedented amount of lakes globally at least once every 21 days. With a high spatial and temporal resolution, SWOT can be used to measure global water storage changes and improve climate modelling. This study contributes to assess the performance of SWOT in observing the Water Surface Elevation (WSE) of lakes, by analysing SWOT observations of Ice Marginal Lakes (IMLs) in southwest Greenland. These lakes are particularly difficult to observe with SWOT because the region is mountainous and the lake surfaces are covered in ice for most of the year. For this purpose, three lakes of different sizes were chosen and the WSEs obtained from the two main SWOT lake data products were compared to elevations from the Ice, Cloud, and land Elevation Satellite 2 (ICESat-2). While SWOTs Pixel Cloud Data Product (PIXC) product contains more observations during the ice-covered period and is better for finding error sources, the Lake Single Pass Vector Product (LakeSP) product is more convenient for analysing large numbers of lakes and both products have a similar accuracy after data editing. The SWOT-derived WSEs obtained in this study are not in compliance with the WSE mission requirements (1σ <10 cm for lakes >1 km^2 and 1σ <25 cm for lakes <1 km^2), because the average WSE difference to ICESat-2 lies between 0.27-1.38 m for the three lakes that were analysed. This analysis indicates that the main error-sources are ice cover - leading to a low Normalised Radar Cross-Section (NRCS) and coherence, phase unwrapping errors and specular ringing - resulting in inconsistent lake outlines. It is recommended that more strict editing should be applied to the SWOT LakeSP product when observing IMLs, in particular regarding ”dark water” pixels, and that the Prior Lake Database (PLD) should be updated to include more ice marginal lakes.

Acronyms

ATL06 ATLAS/ICESat-2 L3B Slope-Corrected Land Ice Height. 13

ATL13 ATLAS/ICESat-2 L3A Along Track Inland Surface Water Data. 13

CNES Centre National d'Études Spatiales. 5

CPU Core Processing Unit. 20

EGM2008 Earth Gravitational Model 2008. 12

GLOF Glacial Lake Outburst Flood. 1

HPC High Performance Computing. 20

ICESat-2 Ice, Cloud, and land Elevation Satellite 2. iii, 1, 13

IML Ice Marginal Lake. iii, 1, 43

InSAR Interferometric Synthetic Aperture Radar. 6

JPL Jet Propulsion Laboratory. 5

KaRIn Ka-band Radar Interferometer. iii, 5

LakeSP Lake Single Pass Vector Product. iii, 2, 13, 43

MAD Median Absolute Deviation. 16, 37

NASA National Aeronautics and Space Administration. 5

NRCS Normalised Radar Cross-Section. iii, 7, 43

PIXC Pixel Cloud Data Product. iii, 2, 10, 43

PIXCVec Pixel Cloud Auxiliary Data Product. 11

PLD Prior Lake Database. iii, 11, 43

SAR Synthetic Aperture Radar. 1, 6

SLC Single Look Complex. 10

STD Standard Deviation. 16

SWOT Surface Water and Ocean Topography. iii, 2, 5, 43

WGS84 World Geodetic System 1984. 13

WSE Water Surface Elevation. iii, 2, 3, 12, 43, 48

Contents

1 Introduction

1.1. Background

Lakes are among the most important components of terrestrial water storage and a key contributor to the water cycle. Monitoring of lake water levels gives us valuable information about human water consumption, industries, irrigation and prevention of droughts, but the distribution of observations is heterogeneous [40][10]. In less populated areas such as Greenland, in-situ measurements of lakes are sparse, and monitoring of lake areas or water levels is largely based on satellite observations. Out of the 30 million estimated natural lakes on Earth (>1 ha), more than 150 000 are located in Greenland [15][14], playing a vital role in transporting and storing meltwater from the Greenland ice sheet. Understanding and quantifying the role of freshwater storage (changes) in global hydrology can help to improve hydrological- and climate models, which is why a good basis of lake observations is important.

Ice Marginal Lakes (IMLs) are characterised by their connection to a glacier or other ice margin, and are therefore often subject to large freshwater influxes and major and frequent storage changes. The more than 10 000 identified IMLs on Greenland play a significant role in the water cycle and pose the risk of creating Glacial Lake Outburst Flood (GLOF) events [14]. Glacier Lake Outburst Floods are natural events, characterised by sudden, large releases of water either from a moraine-dammed or ice-dammed glacial lake [2]. When glacial lakes are dammed by a moraine or glacier with no outlet to the ocean but are filled with meltwater over time, they reach a point of overtopping the moraine or lifting the glacier to create a subglacial tunnel for the water to flow away into the ocean. These unpredictable events can lead to huge amounts of water being drained from the lakes in a matter of hours or days, and pose a risk of flooding downstream environments and changing ecosystems. Historically, GLOFs have been recorded mostly in the Himalayas, where they have caused destruction of dams, farmland and infrastructure on several incidents in the last century [42]. In Greenland, due to increasing meltwater runoff from climate change, the frequency of GLOF events is already increasing, which reduces the inland water storage and increases the freshwater flux to the ocean [14].

1.2. Previous Work

A study by How et al. (2021) [24] combined satellite observations from Sentinel-1 Synthetic Aperture Radar (SAR) imagery, Sentinel-2 optical imagery and the ArcticDEM terrain model to create an inventory of ice marginal lakes in Greenland, including more than 3300 IMLs (>0.05 km^2). However, this inventory only contains the lake outline and area, but not the water level, or changes of lakes over time. While most studies of IMLs focus on one specific lake or small area, Dømgaard et al. (2024) [14] conducted a comprehensive analysis of IML water level changes covering 1300 IMLs in Greenland. By using altimetry data from the Ice, Cloud, and land Elevation Satellite 2 (ICESat-2) and IceBridge ATM missions, water level observations from 2003 until 2023 were combined to detect 541 GLOF events over that period, including lakes with an area >0.2 km^2. Most observations in recent years (2018-2023) were taken by ICESat-2, which produces only one observations roughly every 3 months and does not cover the entire ground surface, thus lakes lying between ICESat-2 tracks are missing from the altime-

try observations. This leaves a gap between the 1300 lakes included in the study and the more than 10 000 IMLs identified by the Danish Agency for Data Supply and Infrastructure [11]. Monitoring the water levels of IMLs is particularly challenging because the surface is often covered with calving ice from a glacier front or surface ice due to low temperatures. Additionally, Greenland consists of very mountainous terrain, posing obstacles for remote sensing methods using side-looking satellites or having a low spatial resolution [39]. A high spatial resolution is essential to distinguish the height of lakes and rivers in this area from their surrounding mountains.

NASA's Surface Water and Ocean Topography (SWOT) satellite mission has the goal to provide high-resolution observations for global hydrology and climate modelling in unprecedented frequency compared to previous missions, such as ICESat-2 with a revisit time of 91 days, which has observed more than 220 thousand water bodies worldwide [41]. SWOT was designed to observe the ocean, rivers and lakes as small as 250 m x 250 m (with a goal of 100 m x 100 m), thereby contributing to close the observation gap of small lakes in altimetry. This provides a new opportunity to improve the observations of surface waters due to SWOTs special frequency range, wide-swath measuring technique and short revisit time of 21 days. Combined, SWOT can observe lakes larger than 1 ha globally between 1-7 times per 21-day repeat orbit (see Figure 1.1) depending on latitude, making it possible to observe the dynamics of terrestrial water storage as well as oceanography.

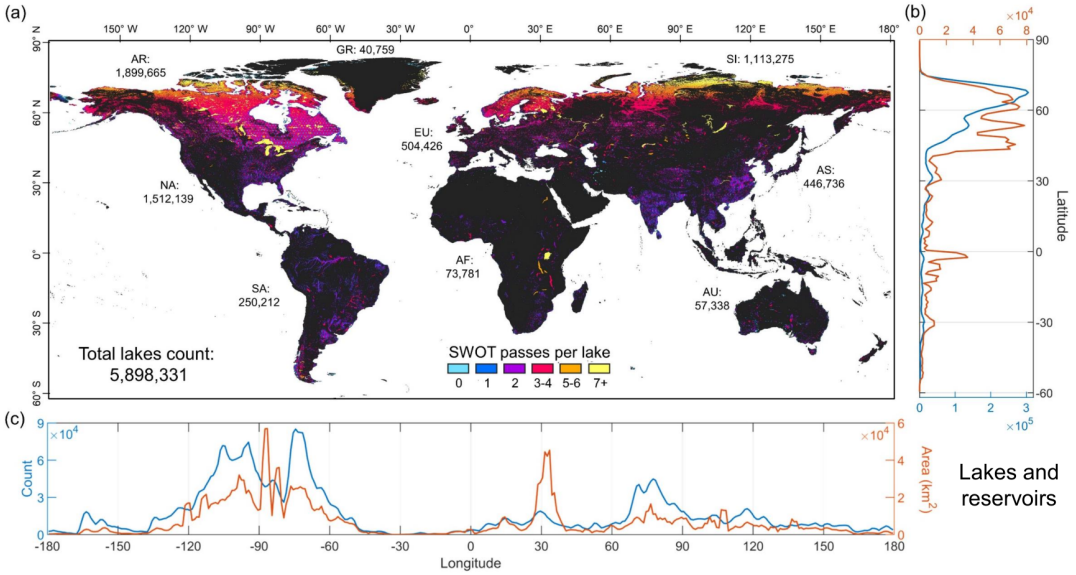

Figure 1.1: Global map (excluding Antarctica) of lakes and reservoirs (a) with colours indicating how often a lake is observed in a 21-day SWOT cycle. (b) and (c) show the water body distribution per latitude and longitude respectively [35].

Launched in December 2022, SWOT has collected approximately two years of data in its science orbit so far and has already delivered promising results in the number of observed lakes and the accuracy of their derived Water Surface Elevation (WSE). According to Wang et al. (2025) [36], SWOT observed 3 million lakes with at least one valid measurement in the first 4 months of its science orbit. A study on water bodies in Australia obtained an accuracy in water surface elevation up to 3-6 cm (for large lakes) with SWOTs Pixel Cloud Data Product (PIXC) product and 24 cm with the Lake Single Pass Vector Product (LakeSP) product [25]. During the calibration and validation phase, initial investigations of the Arzuma reservoir in Burkina Faso have shown that SWOT can obtain accurate water level and lake surface area observations. Here, a 1σ error of 9 cm in WSE compared to in-situ measurements and a 17% difference in lake area compared to Sentinel-2 were found, in line with the mission requirements regarding WSE, which can be seen in Table 1.1.

1.3. Motivation

SWOT contains three data products from which lake WSEs can be derived. The main data product for lakes and reservoirs is the LakeSP product, which provides geometries of all recognised lake features and their WSEs for each SWOT overpass. The lower level PIXC product containing individually ob-

Table 1.1: SWOT mission science requirements and goals for Water Surface Elevation (WSE) of lakes [3].

WSE error	Requirement	Goal
1σ for lakes >1 km^2	<10 cm	
1σ for lakes >250x250 m^2 and <1 km^2	<25 cm	
Lake detection	250x250 m^2	100x100 m^2

served water pixels and the higher level Raster product with gridded data can also be used to obtain water surface elevations of lakes. For gaining a better insight into the processing and underlying data of the LakeSP product, the PIXC product will be analysed in addition to the LakeSP product in this study. By including both of these data products it can also be compared how different processing impacts the obtained WSE estimates and which data product is most suitable for a given application.

As no in-situ measurements of the water level are available for any IMLs in Greenland, other data such as from satellite altimetry are needed to obtain a reference for the water surface elevation accuracy derived by SWOT. Here the ICESat-2 altimetry data is an obvious choice for a height reference because it contains observations during the same time period as SWOT and specifically covers polar regions including Greenland well. This mission has a long record of high-accuracy measurements of surface elevation (better than 3.3 cm bias [6]), including land ice, sea ice, and inland surface water.

If the WSE of IMLs can be obtained from SWOT with a high accuracy and consistency, they could provide valuable information for detecting GLOF events due to SWOTs sub-monthly coverage. Therefore, this study has the purpose to assess the accuracy of the water surface elevations that can be derived from SWOT observations of IMLs in Greenland. Simultaneously, it can be assessed how well SWOT performs under difficult conditions due to Greenlands mountainous terrain and arctic climate. Due to these difficult conditions it is particularly important to identify origins of error causes in the WSE and what can be done to improve the accuracy of the obtained WSE estimates. Identifying causes of errors can be challenging if errors cannot be attributed to a single cause. Therefore, the k-means clustering method will be tested as a solution to find combinations of multiple causes.

1.4. Research Objective

The main goal of this research is summarised in the following research objective:

To assess the performance of SWOT in observing water surface elevation and variability of Ice Marginal Lakes in Greenland

and accompanying sub-questions:

- *When comparing the LakeSP and PIXC data products from SWOT, what are their main advantages and drawbacks with regards to the retrieved lake surface elevations?*
  For users that wish to use SWOT data on lakes it is essential to know which product is most suitable for a given application. For this comparison, the accessibility, computational efficiency, WSE accuracy and consistency will be assessed.
- *How do SWOT-derived water surface elevations of ice marginal lakes compare to those derived from ICESat-2 altimetry data in terms of accuracy and consistency?*
  The accuracy is indicated by the difference between ICESat-2 WSE measurements and the WSE obtained from each of the two SWOT products. The consistency describes the frequency of valid SWOT observations and the WSE variability.
- *What are the main issues for SWOT in detecting water surface elevations of ice marginal lakes in Greenland?*
  It is important to determine what the limitations of the LakeSP and PIXC products are for obtaining more accurate WSE estimates from SWOT. Also, possible errors introduced during observation and processing should be identified in order to reduce the WSE error as much as possible. For

this purpose, individual observations of the PIXC product will be analysed and optical imagery from Sentinel-2 will be included for comparison.

- *How can the water level estimates obtained via different SWOT data products be improved to create reliable records with good accuracy and consistency?*
  For obtaining WSE records of IMLs from SWOT which are reliable enough to be used in other applications, recommendations will be given on how to obtain good quality WSE measurements from each SWOT lake product. These should include solutions to avoid influence from the main observation and processing errors.

To provide the reader with a fundamental understanding of the SWOT mission, an introduction of the measurement principle to obtain water surface elevations from SWOT is given in chapter 2. This is followed by a description of the SWOT and ICESat-2 data which were analysed in this research. In chapter 4 it is described how the WSEs over time of each IML included in this study were derived from the SWOT data products and how they were compared to ICESat-2. Furthermore, the methods used to identify error causes for the WSE are described. Chapter 5 shows the results of the WSEs obtained from the LakeSP product, PIXC product and ICESat-2 as well as the results of the error analysis. Chapter 6 aims to answer the above research questions by interpreting the results and providing recommendations for monitoring water levels of IMLs and improving the SWOT lake products. Last but not least the conclusion will provide a summary of the key takeaways from this research.

2

Introduction to the SWOT Mission

Before describing the two SWOT datasets from which lake water surface elevations are obtained for this study, a brief introduction to the the SWOT mission is given here, where it will be explained how SWOT measures the WSE and what new capabilities SWOT has compared to other altimeter missions.

2.1. Mission Description

The Surface Water and Ocean Topography (SWOT) mission is a collaboration of the National Aeronautics and Space Administration (NASA) Jet Propulsion Laboratory and the Centre National d'Études Spatiales (CNES) to create a global survey of ocean and inland surface water topography through the Ka-band Radar Interferometer (KaRIn) instrument, which is a wide-swath altimeter [21][20][18]. Compared to other altimeters which only obtain elevations of single point lines along the ground such as CryoSat-2, Sentinel-3 and ICESat-2 [16], SWOT has the advantage that it covers a ground track of 140 km width in a single overpass by looking both left and right of the satellite track. In this way, the whole globe can be covered in a repeat orbit of 21 days. A visualisation of the satellite geometry is shown in Figure 2.1, which shows the 60 km swath tracks left and right of the nadir, separated by a 20 km strip, to avoid bright backscatter close to nadir or overlap with the nadir looking point-altimeter.

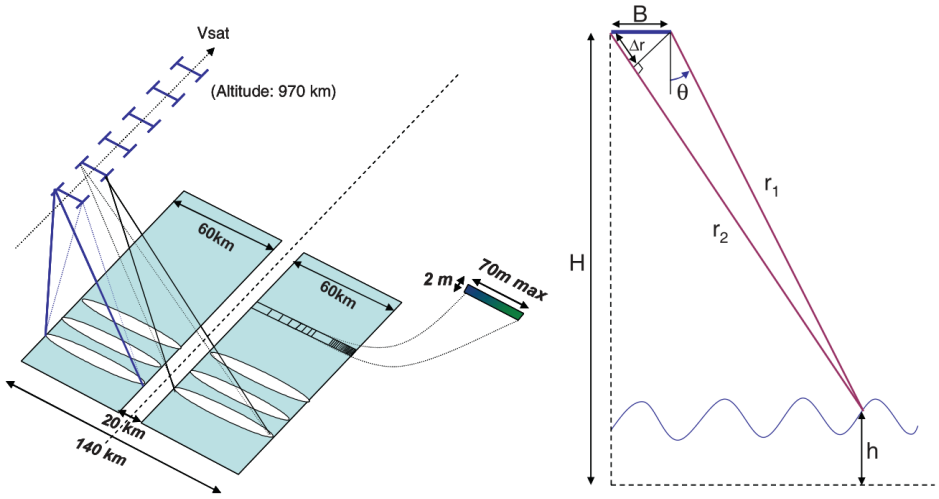

Figure 2.1: KaRIn viewing geometry of the wide-swath altimetry (left) showing the increase of spatial resolution towards the far range. Illustration of the range difference used to calculate the height of ground points (right) [19].

SWOT was launched into a calibration and validation orbit in December 2022. Only in July 2023 it was manoeuvred into the nominal 21-day science orbit, in which it is now at a mean altitude of 905 km above the WGS84 ellipsoid. The orbit inclination is 77.6°, which means that the northernmost region of

Greenland is not observed. Onboard the satellite are the Ka-band Radar Interferometer (KaRIn), dual-frequency (Ku- and C-band) pulse-limited Nadir Altimeter (NAlt), three-frequency Advanced Microwave Radiometer (AMR), Doppler Orbitography and Radiopositioning Integrated by Satellite (DORIS) receiver, Global Positioning System Payload (GPSP) receiver and a Laser Retroreflector Array (LRA) [9].

2.2. KaRIn Measurement Principles

Other satellites using Interferometric SAR imaging, such as Sentinel-1, tend to have one antenna and rely on multiple overpasses to produce one InSAR image. What makes KaRIn special is that it employs two antennas separated by a distance (baseline) of 10 m from each other. When one of the antennas sends out a pulse to either the left or the right ground-swath, the signal which is reflected on the surface is received by both antennas. From the time delay of the response signal the range distance r from the antenna to the target can be estimated:

$$r = \frac{c\tau}{2} \tag{2.1}$$

where c is the speed of light, τ the time delay and the division by 2 comes from the round trip distance to Earth and back. The Doppler effect can be used to determine the position of the target in the along-track direction. If the satellite is flying towards the target, it will have a positive shift in frequency (positive Doppler), and if the satellite is flying away from the target it will have a negative frequency shift (negative Doppler). Because the range is the same for a target closer to the satellite with a lower elevation, than for a target further away with a higher elevation, the key to obtain topographic heights or elevation changes is to use Interferometric Synthetic Aperture Radar (InSAR).

InSAR is a method which combines two Synthetic Aperture Radar (SAR) images taken from different locations and possibly at different points in time. The two antennas of KaRIn each capture a complex SAR image with an amplitude and a phase. By complex conjugating the two SAR images which were obtained simultaneously by the left and right antenna, the complex interferogram is obtained. If the two complex images s_1 and s_2 each have an amplitude A and a phase ϕ, the interferogram s_{21} is defined as

$$s_{21} = s_1^* s_2 = A_1 A_2 \mathrm{e}^{j(\phi_2 - \phi_1)} = A_{21} \mathrm{e}^{j\phi_{21}} \tag{2.2}$$

where A_{21} is the interferogram amplitude and ϕ_{21} the interferogram phase [23]. If both antennas were at the exact same location and received the same backscattered signal from a ground target, the phase difference would be 0 and the images described as coherent. The interferogram phase is the phase difference that arises because the range of the two antennas is different for a side-looking geometry. The difference in range, as illustrated on Figure 2.1 is thus given by [19]:

$$\Delta r = \frac{\lambda}{2 \cdot 2\pi} \Phi \tag{2.3}$$

Here, the division by two comes from the round-trip of the phase, while the range difference is only the one way distance. λ is the Ka-band wavelength (8.4 mm) and Φ the unwrapped interferometric phase, which is found from:

$$\Phi = n \cdot 2\pi + \phi \tag{2.4}$$

The interferometric phase measured between the two antennas ϕ is also called the wrapped interferometric phase, because it is obtained as a modulus of 2π radians. To determine the range difference Δr, it is necessary to estimate the integer phase ambiguity number n which determine how many full wavelengths make up the range difference. This results in an ambiguity height h_a corresponding to a phase change of 2π radians.

$$h_a = \frac{\lambda r \sin\theta_{look}}{B \cos\theta_{inc}} \tag{2.5}$$

Here the incidence angle θ_{inc} is the angle between the normal vector of the ground and the range vector, while the look angle θ_{look} is between the satellite nadir-looking vector and the range vector to take the curvature of the Earth into account. If the terrain is not known with an accuracy of $h_a/2$ a priori, spatial unwrapping can be used over a group of pixels, which are expected to have a phase difference of less than $\pm\pi$ to their neighbours. For lakes with a relatively flat surface this approach can be used to spatially unwrap the phase over the lake before the absolute ambiguity is resolved for the entire lake. By integrating the phase of the pixels in the cross-track direction and adding or subtracting one phase cycle when the difference between two adjacent pixels is larger than $\pm\pi$, the relative spatial unwrapping makes use of the assumption that the phase is varying slowly with respect to the cross-track distance from the satellite. The process of finding the correct number of phase ambiguities n and adding them to the wrapped phase to obtain the unwrapped phase is called phase unwrapping.

When looking at the satellite geometry on Figure 2.1, the range difference can also be expressed as:

$$\Delta r = r_2 - r_1 = B \sin(\theta) \tag{2.6}$$

Where θ is the look angle shown in Figure 2.1 (right) and B the baseline. Combining Equation 2.3 and 2.6 gives the following expression for the look angle:

$$\theta = \arcsin\left(\frac{\Phi\lambda}{B4\pi}\right) \tag{2.7}$$

Once the look angle θ is calculated, it is possible to determine the height of the ground point h with respect to the reference surface:

$$h = H - r\cos(\theta) \tag{2.8}$$

The satellite altitude H with respect to the reference surface such as the WGS84 ellipsoid and range r from the center of the satellite to the ground point is obtained from the GPS and travel time respectively.

2.3. Physical Phenomenon and Error Sources

KaRIn operates at the Ka-band frequency with a wavelength of $\lambda = 8.4$ mm, which is shorter than other radar altimeters. This has the advantage that the range difference can be resolved in more detail. However, this also makes phase unwrapping more difficult because the ambiguity height is smaller. By utilising the Ka-band frequency, even higher image resolution (approximately 5 m in azimuth and 0.75 m in slant range) than C- or X-band SAR missions such as Sentinel-1 (spatial resolution of 20 m by 5 m) can be achieved [9][12]. Another advantage is that using a smaller wavelength allows for a smaller baseline between the antennas and thus a more compact satellite design, whereas using C- or X-band radars require a much larger separation distance between the antennas, such as 60 m for the Shuttle Radar Topography Mission (SRTM) [3]. One of the drawbacks of a smaller wavelength is that the signal is attenuated faster, and therefore the measurements are more sensitive to atmospheric conditions. While radar altimeters are excellent for penetrating cloud cover, the Ka-band measurements are more sensitive to rain and blowing snow than altimeters operating at longer wavelengths [19]. This could be an additional issue for measurements in Greenland.

Two important parameters for working with SAR images are the coherence and Normalised Radar Cross-Section (NRCS) (or σ_0). Coherence is a measure of how similar the two SAR images are and how much random noise is in the interferogram. A good coherence means that the phase difference between the two acquired images does not possess any random noise, while a bad coherence means that the phase differences are randomly distributed between 0 and 2π. The average power reflectivity or scattering coefficient per surface area is characterised by σ_0. It is related to the power of the backscatter

received by the antenna. Often, an area for which the observed σ_0 is high is described as bright, while an area with a low σ_0 is described as dark.

The look angle θ of the KaRIn instrument is very small (1-4°) compared to other SAR systems, which typically have angles between 20-40° [19], meaning that the KaRIn instrument looks very close to nadir. This is an advantage when observing inland water, which generally has a lower surface roughness than land, because a small incident angle means that more of the signal will be reflected back in the direction close to the satellite and not away from the satellite, as would be the case for larger look angles. In this way, a decent backscatter signal from water surfaces can be obtained, which is needed to determine the surface properties. On the other hand, such a small look angle is more prone to layover from surrounding topography, which occurs if the terrain slope is larger than the look angle [39]. As seen from the dashed range lines in Figure 2.2, a point located closer to nadir at a lower elevation and a point further away at a higher elevation have the same range distance to the satellite. When the antenna receives a backscatter signal from the whole area, the travel time can be used to calculate how far away each point is, but if the slope is larger than the look angle, the point seems nearer to the satellite and the signal ends up overlapping with the signal from the points closer to the antenna. Layover also causes shadowing of the area behind the mountain in Figure 2.2, which then cannot be observed.

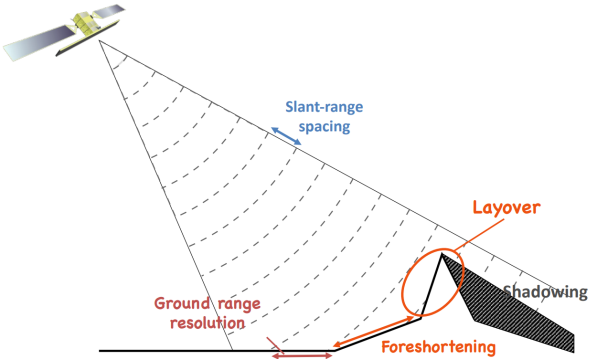

Figure 2.2: Illustration of layover effect. P. L. Dekker, TU Delft [13].

While the area behind a mountain will be shadowed, the side facing the satellite will show up shortened in the SAR image, because the sloped surface spans fewer pixels in the range direction (thus called foreshortening). Additionally, more of the signal is reflected in the direction of the satellite, such that these slopes often appear brighter than the surface would be otherwise. This can also lead to a bright reflection from a sloped land surface being wrongly classified as inland water because inland water surfaces are expected to appear brighter than the surrounding land. As stated in Fjørtoft et al. (2010) [19], any terrain feature, such as a mountain next to an observed lake, with a slope exceeding 1° in near range and 4° in far range, will produce layover and thereby distort the lake water surface elevation. In mountainous areas such as Greenland, a slope larger than 4 degrees is not uncommon and can have serious impacts on observing lakes and rivers located down in the valleys. It is therefore important to take potential layover influence into consideration in this analysis.

Apart from layover, other known error sources for SWOT data are specular ringing and phase unwrapping errors. Specular ringing is a phenomenon caused by bright backscatter from points close to nadir, such as flat water surfaces. When the signal is compressed in the range direction, the response signal has side lobes which extend away from the point source in the across track direction. Usually, the the σ_0 of the side lobes is several orders of magnitude lower than the σ_0 of the surrounding landscape, but when targets at nadir become very bright compared to the rest of the observed area, the side lobes also appear brighter than the surrounding landscape. This can create stripes of high σ_0 in the images, which are then classified as water surface belonging to an intersecting lake. Phase unwrapping errors occur if the wrong number of phase ambiguities is added when unwrapping the phase, which can then result in a wrong location and height of a given pixel. This can happen if the initial height estimate that is used to perform the unwrapping is not accurate enough or the spatial unwrapping does not use a fitting area. For IMLs in Greenland it is possible that mountains surrounding a lake are then included in the same spatial unwrapping region as a lake, even though they have a much higher elevation.

3

Data Description

3.1. Selecting the Area of Interest

In this study, the southwest basin of Greenland was chosen as the area of interest, since this area experiences some of the highest melt rates in Greenland and has a large number of ice marginal lakes according to Dømgaard et al. (2024) [14]. Out of all IMLs in southwest Greenland, three lakes of varying sizes were chosen for an in-depth study and compared to ICESat-2 observations for reference. The three lakes were selected because i) for most of the overpasses a WSE was computed in the LakeSP product, and ii) they were covered by at least one ICESat-2 track. The location of the study area and of these three lakes can be seen in Figure 3.1 including an ortophoto of each lake from the Danish Agency for Data Supply and Infrastructure [11] (on different scales). The lake with the number 1 is unnamed with an area of 5.5 km^2 which will be referred to as the medium-sized lake. The largest of these three lakes is the lake Isortuarsuup Tasia with 55 km^2, which is number 2 on the map. Number 3 is the smallest lake with a size of 0.2 km^2, which is also unnamed. The small lake is located 400 km south of the medium-sized lake and 230 km south of the lake Isortuarsuup Tasia. By focusing on three lakes of varying sizes, locations and elevations, an in-depth study was performed to compare the two SWOT lake products and determine main error causes.

This research used data from the SWOT Level 2 High Rate Water Mask Pixel Cloud Data Product (PIXC) as well as the SWOT Level 2 KaRIn High Rate Lake Single Pass Vector Product (LakeSP). Both of these products provide data from individual satellite overpasses but the PIXC product contains more detailed information than the LakeSP product. Therefore, data from the LakeSP product was downloaded for the whole region of southwest Greenland (44-54°W, 60-69°N), while PIXC data was only downloaded for the three chosen lakes.

Additionally, a fourth lake was included in the analysis initially, which is called lake Hullet and is located at the southern tip of Greenland. This lake had to be discarded from the analysis because SWOT was not able to detect it properly, but a few examples of this lake were still included in the report to show what caused SWOT to wrongly detect this lake.

3.2. SWOT Pixel Cloud Data Product

The PIXC product is separated into files covering an area of 64 km x 64 km, where each file belongs to one satellite pass of the left or right swath and contains around 5-10 million pixels. Because the goal is to observe lakes as small as 100 m x 100 m, the high rate mode of SWOT has a pixel spacing of approximately 20 m in the along track direction and 10-70 m in the cross-track direction, resulting in data files of around 1 GB per file. The data is available for free via NASA's Earthdata portal in NetCDF format. In this project, all PIXC data files covering one of the three chosen lakes were retrieved for the period November 2023 to February 2025. The data was downloaded by finding the coordinates of the three lakes and downloading all datafiles in the given period which cover those coordinates. Each lake comprised of around 100 GB of data.

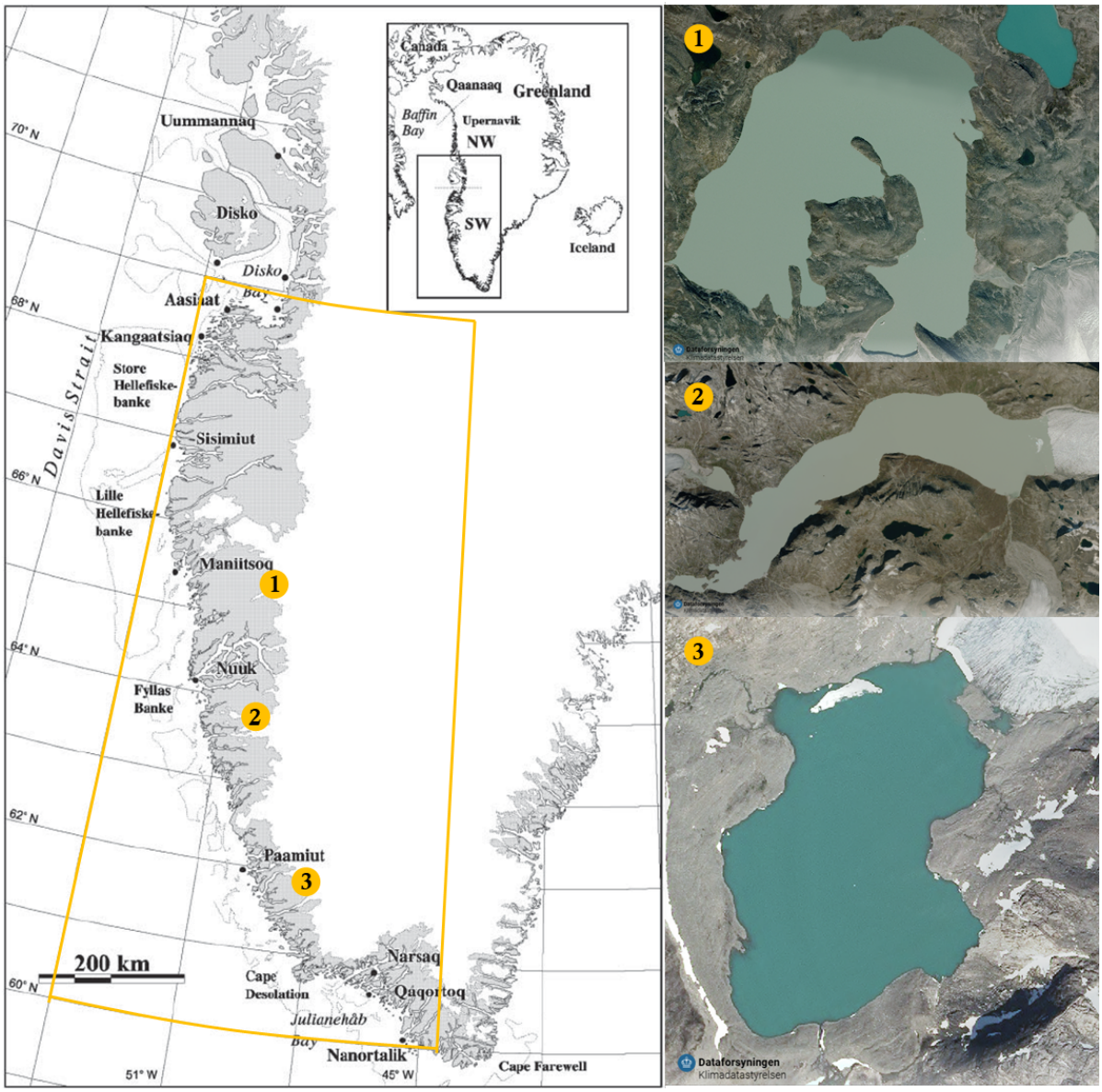

Figure 3.1: Map of southwest Greenland, where the area of interest is marked in orange and the locations of the three chosen lakes are indicated with numbers [4]. On the right an ortophoto of the (1) medium-sized lake, (2) lake Isortuarsuup Tasia and (3) small lake is shown [11].

PIXC includes geolocated heights of all observed terrestrial water pixels and a multitude of properties such as the complex interferogram, correction factors, classification and quality flags for each pixel [7]. The pixels are classified into seven categories, shown in Table 3.1, based on the level 1 Single Look Complex (SLC) product and additional data on water occurrence. Open water is expected to have a high backscatter (σ_0) and high coherence compared to the surrounding land, therefore classes 3 and 4 are the areas with the highest quality of water detection. Classes 1 and 2 are to mark land pixels, which are included either because they lie close to water, or because they have a high backscatter in SWOT, but are identified as land or ice in the auxiliary data. Classes 5-7 indicate less good quality, because these pixels are either identified as dark water, meaning they have a low backscatter (class 5) or as low coherence water (classes 6 and 7). Pixels in these three classes are best avoided, because the geolocations and heights derived from them have shown significant noise and artifacts [37]. The reason these pixels are identified as water is the external information on the probability of water being present, even if no presence of water is detected by the satellite.

The geolocation flag `geolocation_qual` is a particularly valuable quality indicator because it is a

Table 3.1: The `classification` variable of the PIXC product contains an integer value from 1 to 7 indicating which of these classes the pixel is categorised as [9].

Class	Definition
1	Land
2	Land near water
3	Water near land
4	Open water
5	Dark water
6	Low-coherence water near land
7	Open low-coherence water

bitwise flag indicating possible issues with the calculated geolocation. Each possible issue is assigned a value, from the least significant issue having a value of 2^0 to the most significant issue having a value of 2^{31}. The value of each pixel is the sum of flagged issues, making it possible to mark multiple issues in one value and distinguishing which issues apply by simple reverse calculations. Values of 2^0, 2^1 and 2^2 tell, respectively, that the layover is significant, the phase noise is suspect, and the phase unwrapping is suspect. If all these three are the case, a total value of $2^0 + 2^1 + 2^2 = 7$ would be assigned to the pixel. If a pixel has no issues, the value becomes 0 and the geolocation is known to be reliable. A table of all possible issues is shown in Figure A.2 sorted by severity. The binary quality flag `sig0_qual` indicates the quality of the σ_0, with 0 indicating good quality and 1 indicating bad quality.

Two other parameters which were included in the analysis are the height sensitivities to the phase and the range. The height to phase sensitivity describes how much the height changes per radian of phase change, while the height to range sensitivity describes how much the height changes for a one meter change in range. The height to phase sensitivity is similar to the ambiguity height if we divide by 2π (a full phase cycle):

$$\frac{dh}{d\phi} = \frac{\lambda r \sin\theta_{look}}{2\pi B \cos\theta_{inc}} \tag{3.1}$$

If the height to phase sensitivity is high, a small phase error can lead to a large height error, but since the sensitivity differs in the across track direction, this variable can also show how a phase error will affect different areas of the image. The height to range sensitivity works similarly but for the range instead.

This product can be used in combination with the Pixel Cloud Auxiliary Data Product (PIXCVec) to extract pixels by their assigned lake id because the PIXCVec product utilises the LakeSP product to assign a lake id to each pixel corresponding to the lake identified in the Prior Lake Database (PLD). In case this approach fails because the PLD is not sufficient or because the lakes cannot be extracted from the observation, employing the PIXC product offers a different method for observing lakes than the LakeSP product. By using the PIXC product in combination with lake outlines from an ice marginal lake dataset as boundary, only the pixels located within the desired lake are extracted.

3.3. Background on how the LakeSP Product is Produced

Before describing the LaksSP data used in this study, it is beneficial to understand how the water surface elevations in the LakeSP product were obtained such that they can be recreated from the PIXC product and compared to the LakeSP product. Below, it is described how the LakeSP product was derived from the PIXC product in combination with the PLD by the data providers (CNES and JPL) according to the LakeSP product description [30].

Initially, the water pixels intersecting river reaches which are identified in the SWOT river database are removed in order to obtain only water pixels which belong to lakes and not to rivers. The remaining pix-

els are aggregated into lake geometries using the PLD and processed into three different sub-products as shown in Figure 3.2 [36]:

- observation oriented lake geometries intersecting water features present in the PLD,
- PLD-oriented lake geometries, where observed lakes are assigned to pre-identified lakes,
- unassigned features not identified in the river or lake databases.

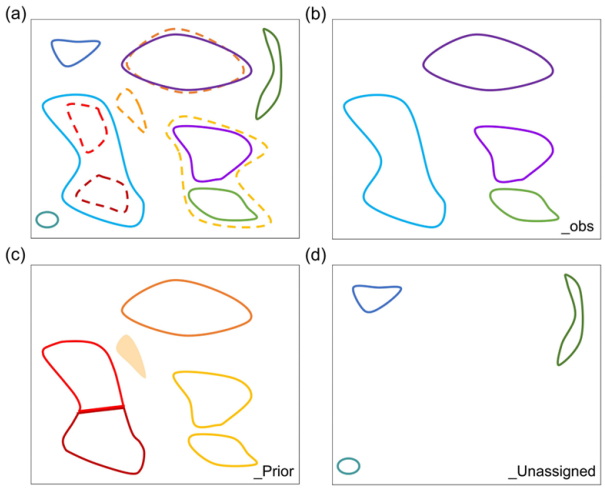

Figure 3.2: Illustration of the three LakeSP product results, where (a) shows the observed water features (solid) along with lakes in the PLD (dashed), (b) shows the observation oriented (LakeSP_Obs) product, each colour represents a different water feature. (c) shows the PLD-oriented (LakeSP_Prior) product and (d) the unassigned features in the LakeSP_Unassigned product [36].

This project focuses on the PLD-oriented product, which uses the observed water features to assign them to existing lakes in the PLD and should therefore provide the most consistent lake features over time. The observation-oriented product uses the PLD to know where water is expected, but does not assign water features to the lakes already existing in the PLD. Instead, the water features are recorded in the shape that they are observed in. This product could have been chosen to obtain lake features most in line with the actual satellite observations.

For each lake, the identified pixels from the PIXC product are used to determine the observed lake outline, lake area and Water Surface Elevation (WSE) as primary variables of the LakeSP product. The WSE in the LakeSP product is the mean height-constrained height of all pixels in the lake. The height-constrained geolocation for each pixel in the lake is calculated to reduce the geolocation noise, and thus obtain a more precise height and location estimate. By assuming that all pixels of one lake observation should have roughly the same surface elevation, a target height is computed, which is used to constrain the geolocation of each pixel. This is either obtained from calculating an uncertainty-weighted average height or fitting a polynomial model to the pixel heights across the lake, if the water body is large enough to experience height variation. As described in chapter 2, the known range to the target pixel and its Doppler create a circle with the satellite in the center, along which the point can be moved. The target height directs where we have to move along the range circle to obtain the expected height of the pixel. Because the height and the coordinates are connected, the coordinates of the height-constrained geolocation will also be different than the previous coordinates of the pixel.

The uncertainty-weighted average surface elevation is calculated as follows:

$$WSE_{mean} = \frac{\sum_p w_p \cdot WSE_p}{\sum_p w_p} \tag{3.2}$$

where w_p are the weights of each pixel calculated from the height STD of each pixel $w_p = 1/\sigma^2_{wse,p}$. WSE_p is the height-constrained height of each pixel with reference to the EGM2008 geoid model, which is calculated as follows:

$$WSE_p = H - geoid\_hght - solid\_tide - load\_tide\_fes - pole\_tide \tag{3.3}$$

Where H is the geocentric height of the water surface with respect to the WGS84 ellipsoid taken from the PIXC height. The geoid height `geoid_hght` is the height of the provided geoid model in meters above the reference ellipsoid, and the other three terms are corrections for tidal effects. The three tide corrections are based on models and remove the solid earth tide (`solid_tide`), load tide (`load_tide_fes`) and pole tide (`pole_tide`) components from the observed height. Corrections for media (atmospheric) delays are already taken into account in the PIXC height. This WSE_{mean} is then applied as the target height to compute the height-constrained geolocation of each pixel in the lake, which are used to calculate the mean WSE of the lake.

3.4. SWOT Lake Single Pass Vector Product

The LakeSP product consists of lake features in the form of shape files and include information such as the lake area, water surface elevation and geolocated lake geometries. From the layover error of each pixel in the PIXC product, the mean layover error was included in the LakeSP product. Each datafile contains the identified water features of one full swath (both left and right side of one overpass) over one continent area. Since Greenland was assigned its own continent area, data from four SWOT tracks over Greenland was downloaded, which extend in 128 km wide strips across Greenland. These four tracks are part of different orbits during SWOTs 21-day cycle, and are thus obtained on different days. They were chosen because they collectively cover the study area of southwest Greenland and also contain many overlapping areas, to achieve the highest possible frequency and number of observations for this study. All available overpasses from those four tracks were downloaded over the period November 2023 to February 2025. The filesizes are around 50 MB, making this product favorable for investigating larger areas or longer time periods.

In addition to the measured hydrological parameters, several quality indicator variables are given in the lake product in the form of quality flags [29]. The `quality_f` variable gives an overall indicator for the observation quality, it is 0 if more than 70% of pixels in the observation were good and 1 otherwise. The ice cover flag `ice_f` is 0 if the lake is ice-free, 1 if there is partial or uncertain ice cover and 2 for full ice cover. The ice cover classification is based on an empirical model of ice conditions from 2010-2020, and indicates the expected ice cover conditions for a given lake [36]. The dark water flag `dark_frac` indicates the percentage of the lake pixels which are classified as ”dark water”, either due to low backscatter or because it is not really detected as water [9]. Last but not least is the quality flag of the cross-over calibration `xovr_cal_q`, where 0 is good, 1 is suspect, and 2 is bad.

3.5. ICESat-2 ATL06 Product

The ATLAS instrument aboard the Ice, Cloud, and land Elevation Satellite 2 (ICESat-2) is a photon-counting lidar altimeter [33], measuring the time it takes for a laser pulse to travel from the instrument to the Earth and back. It has three pairs of beam tracks, to the left, center and right of the nadir, which are separated by approximately 3 km in the across track direction. Each pair has a weak and a strong beam (left and right) separated by approximately 90 m in the across-track direction [8]. ICESat-2 measurements are available since October 2018.

Because ICESat-2 has a 91-day repeat orbit and individual beam tracks, it will not cover all lakes observed by the SWOT wide-swath altimeter, and observed lakes will have fewer overpasses, roughly one every three months from one ICESat-2 track. However, lakes which are covered by multiple ICESat-2 tracks are able to obtain more frequent WSE observations. This is an advantage when comparing the WSE measurements of one lake from SWOT to ICESat-2, because SWOT is able to obtain more observations in time than ICESat-2. It has to be noted that the ICESat-2 observations can have large time differences to the SWOT observations they are being compared to. Therefore, ICESat-2 cannot provide real-time validation for the SWOT WSEs. The location of the ICESat-2 tracks could be identified via the web portal OpenAltimetry [26].

The ATLAS/ICESat-2 L3B Slope-Corrected Land Ice Height (ATL06) product of ICESat-2 has a much better coverage than the inland surface water ATL13 product, and also covers large amounts of land

and lakes in Greenland [32]. That is why the ATL06 product was preferred to the ATL13 product in this project to maximise the amount of available reference observations.

The ATL06 product is stored in HDF5 files with one file covering 1/14th of an orbit for one pass. Included for each of the six ground tracks are the land ice height, residual histogram and quality assessment of the observation. The land ice height is given as the mean surface height averaged along 40 m of ground track, which is sampled every 20 m. Through precise orbit determination using GPS, the latitude, longitude and height is found with reference to the WGS84 ellipsoid. This reference is the same as for the PIXC product and can easily be derived from the LakeSP product. As part of this study, ATL06 data from the period August 2023 – February 2025 for all available overpasses intersecting each of the three lakes was downloaded. The coordinates of each lake were used to download all datafiles covering these coordinates. Each datafile contains the measured height, coordinates and several quality indicators of each sample point along the three beam pairs.

The quality flag `atl06_quality_summary` indicates the overall quality of a data point based on four characteristics, where 0 means no likely problems and 1 means one or more likely problems are encountered. The four characteristics are given in Table 3.2, where the threshold defines when the quality can be accepted as good. PE stands for Photon Events, which are the photons returned to the ICESat-2 detector. Apart from this, several other quality flags are given, to indicate the impact of blowing snow or clouds, which can have an impact on the photon-scattering. The Multiple Scattering Warning flag `msw_flag` provides a summary on these other quality flags, and will be used for simplicity. Two error

Table 3.2: Overview of the four requirements which all need to be fulfilled for the quality summary to receive a value of 0 [33].

Characteristic	Threshold	Description
`h_li_sigma`	<1 m	Errors in surface height are moderate or better
`snr_significance`	< 0.02	Surface detection blunders are unlikely
`signal_selection_source`	<= 1	Signal selection must be based on ATL03 photons
`n_fit_photons/w_surface_window_final`	>1 PE /m for weak beams, >4 PE/m for strong beams	The vertical density of photons in the final surface window.

sources which cannot be corrected for in processing are Atmospheric forward scattering and subsurface scattering. If the atmosphere is cloudy, photons may be scattered but still reach the surface and return to the satellite with delay. This results in a lower estimate of the surface elevation because the time delay determines the distance to the ground. Similarly, photons may be scattered inside an ice or snow surface before returning to the satellite, which also leads to a lower estimated surface elevation.

The main features of the three different types of satellite data used in this analysis are summarised in Table 3.3 for comparison.

Table 3.3: Main features of the three data products included in this study with emphasis on the main differences.

	SWOT PIXC	SWOT LakeSP	ICESat-2 ATL06
observational record	since Nov. 2023	since Nov. 2023	since Oct. 2018
repeat orbit	21 days	21 days	91 days
coverage	140 km wide swath	140 km wide swath	3 groundtrack pairs
Instrument	KaRIn (radar)	KaRIn (radar)	ATLAS (laser)
data format	pixel cloud	lake geometries	pixel tracks

4

Methodology

In this chapter it is described how the SWOT and ICESat-2 data were processed to obtain the WSE for all IMLs in southwest Greenland from the LakeSP product and to obtain the WSE for the three selected lakes from the PIXC product and ICESat-2 ATL06 product.

Initially, the LakeSP data was used to analyse all IMLs in the area of interest to find out how many IMLs are observed by SWOT and which errors occur in the LakeSP product. Furthermore, three lakes were selected for which the SWOT-derived WSE was compared to ICESat-2 elevations. Because the LakeSP product alone cannot answer what is causing the errors in the WSE, the PIXC product was included in addition to the LakeSP product. The WSE derived from the PIXC data was compared to the WSE from the LakeSP data and ICESat-2, and a detailed error analysis was performed on the PIXC data. Finally, all WSE results of the three lakes were compared quantitatively to assess the accuracy of SWOT in observing water surface elevations of IMLs.

4.1. Derive WSE Time Series from the LakeSP Product

For all IMLs in the area of interest, which are present in the LakeSP product, a time series of the SWOT-derived WSE was created. The process of extracting WSE estimates from the LakeSP product and comparing them to ICESat-2 is summarised in Figure 4.1. As a first step of assessing the water surface elevation in the LakeSP product, all observations of IMLs were extracted from the LakeSP data. The inventory of ice marginal lakes from How et al. (2021) [24] was utilised to extract the IMLs on a basis of spatial intersection. Next, the data over the whole time period was combined for each lake in the LakeSP product.

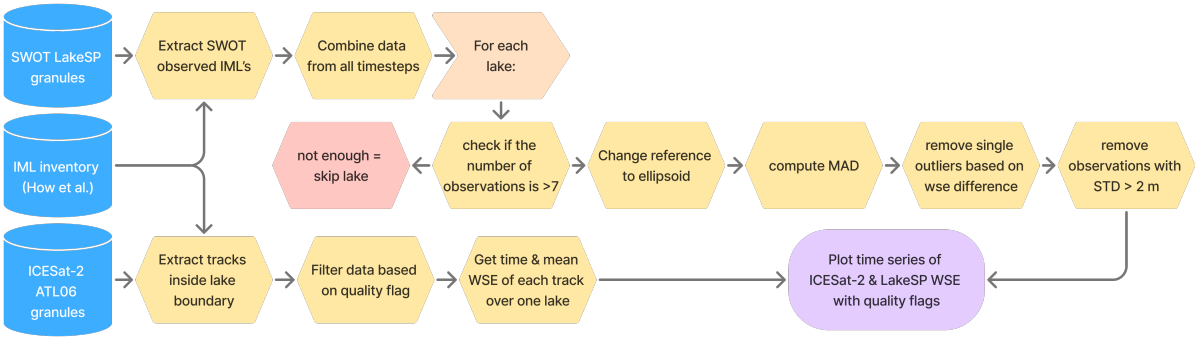

Figure 4.1: Flowchart of the LakeSP processing to obtain water surface elevations and compare them to ICESat-2 elevations. The process for ICESat-2 is only performed for the three chosen lakes. The flowchart was created with Figma [17].

4.1.1. Remove SWOT Observations Affected by Specular Ringing

To compare the ice marginal lakes detected by SWOT to those in Dømgaards and Hows datasets, maps of the lake locations and outlines were created. These maps can also show impacts from specular ringing or errors in the geolocation on the lake outlines and locations. To avoid errors from specular ringing in the SWOT dataset, the lake geometries from How et al. (2021) were used to replace the geometries from the SWOT observations. If a lake observation has an area larger than the largest lake in southwest Greenland (which has an area of 73 km^2), that observation of the lake was removed from further processing. Furthermore, assessing the variability of lake surface elevation becomes unreliable if too few observations are present, therefore lakes with fewer than 8 observations were removed from the data.

4.1.2. Indicate Data Quality with Flags

Ideally, one should also remove observations identified as bad quality, indicated by the quality flags in the data. In the case of ice marginal lakes in Greenland, doing this would remove up to 89% of the observations, which is why this part of the processing was omitted. Instead, the quality flags were used to mark potential problems with the data when plotting the time series of water surface elevation for each lake. The summary quality flag `quality_f` was used to mark observations where the overall quality of the observation is not good (these have the value 1). The observations of lakes partially or fully covered in ice were flagged with the `ice_f` flag and have a value of 1 or 2, respectively. Additionally, the observation was flagged if more than 85% of pixels in the observation were classified as dark water, meaning a dark water fraction of more than 85%, and if the observation has a suspect or bad crossover calibration indicated by the `xovr_cal_q` flag.

Since ICESat-2 measures the elevation with reference to the WGS84 ellipsoid, and the ATL06 product does not contain elevations wrt. the geoid or geoid heights above the ellipsoid, a reference change had to be performed on the LakeSP elevations, to change their height reference from the EGM2008 geoid to the WGS84 ellipsoid. This was done by adding the geoid height, which is given in the LakeSP product, to each WSE observation.

4.1.3. Assess Uncertainty Through the MAD

As a robust method of calculating variability against the influence of outliers, the Median Absolute Deviation (MAD) was calculated for each lake over the whole time period. This method of estimating variability is more robust against outliers than the Standard Deviation (STD). The MAD was calculated as follows:

$$\mathrm{MAD} = \mathrm{med}(|\mathrm{WSE}_i - \mathrm{med}(\mathrm{WSE})|) \tag{4.1}$$

Where WSE_i is the observed WSE at each time step in the LakeSP data and $\mathrm{med}(\mathrm{WSE})$ is the median WSE of all time steps.

Based on this, time series with the water surface elevation, indicators for quality flags and the MAD over the entire period were obtained for all observed ice marginal lakes in southwest Greenland.

4.2. Error Analysis Based on LakeSP

As a first step of the error analysis, a histogram of the MADs from all IMLs was plotted. Here, the MAD represents the WSE uncertainty between observations as an alternative to the STD. Each of the IMLs in the LakeSP product with a valid time series was represented by one MAD of the WSE over time. Because only very few observations possessed an MAD larger than 20 m, the MAD-axis was cropped to 20 m to clarify the distribution of smaller MAD values.

Furthermore, the Pearson Correlation coefficient r was computed for eight parameters of the LakeSP data in relation to the MAD: the total lake area, detected lake area, distance from nadir, layover error, number of observations, ice cover flag, dark water fraction and crossover calibration flag. For each of these parameters, the average value of all observations of each lake was taken, therefore it is possible for quality flags to produce non-integer values. Correlations between the MAD and the eight parameters were analysed based on all IMLs. The total and detected lake areas can indicate whether the MAD is

correlated to the (observed) size of the lake. The total lake area includes the detected water area as well as the area which is classified as water based on prior water probability data. Calculating the correlation between the MAD and the distance from each lake to nadir could provide a clue on errors coming from the look angle, backscattering or similar properties related to the viewing geometry, while the layover error can tell us more about the effect of the terrain on the MAD. Apart from the three quality flags for ice cover, dark water classification and cross-over calibration, the correlation between the MAD and the number of observations of each lake was calculated as well. This can give an indication whether a higher number of observations can reduce the WSE uncertainty or not. It would be expected that lakes with less observations have a higher MAD because single outliers will have a large influence, while lakes with more observations should possess more observations close to the median, showing more stable time series.

4.3. Comparison to ICESat-2 WSE

Out of all detected IMLs, only the three chosen lakes were compared to ICESat-2 observations for reference. By selecting only the points within the lake geometry of the corresponding ice marginal lake from Hows dataset, the amount of ICESat-2 points was reduced significantly. In Figure 4.2 the lake outlines are shown together with the ATL06 heights from the available ICESat-2 tracks for each lake.

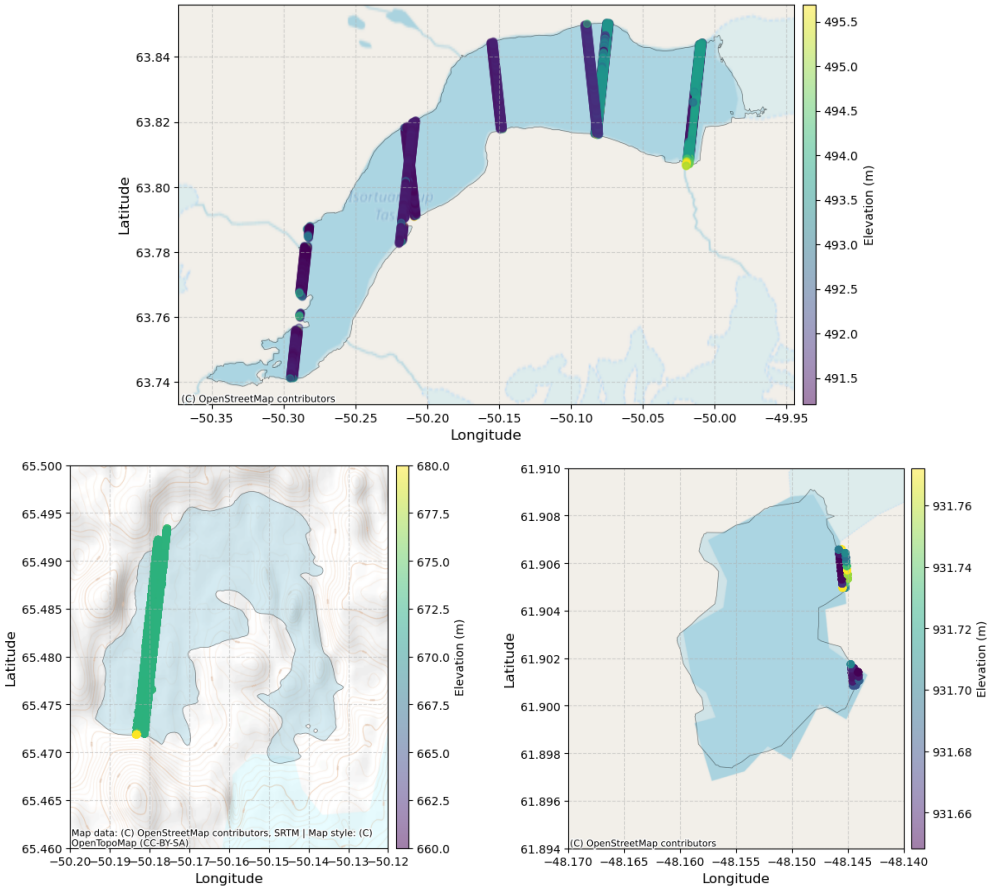

Figure 4.2: Maps of the lake Isortuarsuup Tasia (top), medium-sized lake (bottom left) and small lake (bottom right) with overlying points from all ICESat-2 tracks covering the lakes. The colour of the points indicates the ICESat-2 measured elevation. Note that the maps are not on the same scale.

The large lake Isortuarsuup Tasia (top) is covered by three ICESat-2 tracks (including 7 beam pairs in total), and thus has more observations in time to compare to the SWOT-derived elevations, while the medium (bottom left) and small lake (bottom right) are only covered by one beam pair each.

Additionally, the quality flag `atl06_quality_summary` was used to remove data points with one or more likely problems. By plotting the ”multiple scattering warning” flag it was found that the data over

the lakes were not affected by any blowing snow or cloud cover, therefore no further quality flag data editing needed to be applied in this instance.

For each ICESat-2 pass, the date and median elevation of the pixels covering the lake were extracted and plotted in a time series together with the LakeSP WSEs referenced to the ellipsoid height. Further data editing was applied to the LakeSP data based on Dømgaard et al. (2024) and Maubant et al. (2025) [14][25] to remove outliers in the time series. Therefore, all observations with a STD in height >2 m and a layover error >1 m were removed. The STD present in the LakeSP product declares the uncertainty in height between pixels of that particular observation. For the medium-sized lake a stricter threshold of STD >1 m was applied, because outliers with a low STD were present. The ice-free period is indicated with a green or blue background in the time series. It was determined by inspecting Sentinel-2 optical images for each of the three lakes in this analysis. Since the optical images are not available on a daily resolution, and the lakes can experience several days of partly ice cover, the exact day on which the lake becomes completely ice free had to be estimated.

4.4. Derive WSE Time Series from the PIXC Product

The WSE for the PIXC product was derived for the three chosen lakes in accordance with the documentation of the LakeSP processing, therefore the WSE time series of the PIXC product was obtained similarly to the WSE time series of the LakeSP product. A summary of the processing is shown in Figure 4.3. To increase the processing efficiency, the first step was to exclude all SWOT pixels outside the lake of interest.

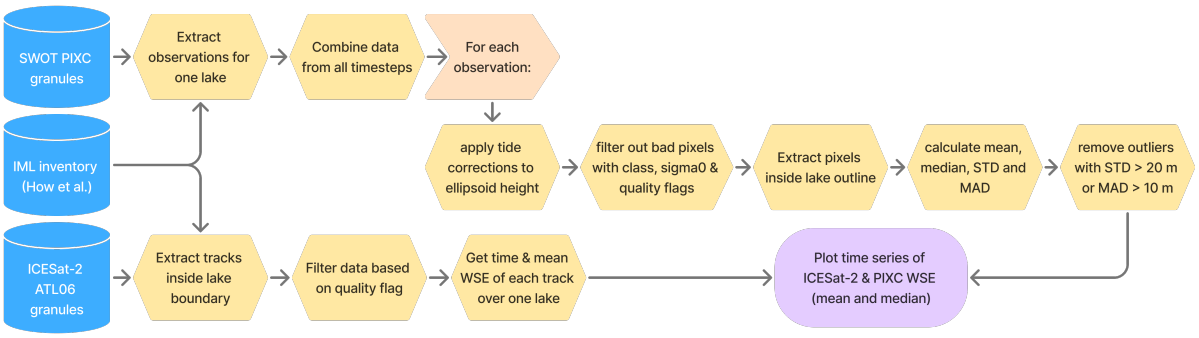

Figure 4.3: Flowchart showing how the PIXC product is processed to obtain the mean and median WSE and compared to ICESat-2 elevations. This whole process was only performed for the three chosen lakes. The flowchart was created with Figma [17].

By utilising the `classification` variable in the PIXC dataset, pixels which are classified as ”land”, ”dark water” or ”water with low coherence” were removed from the data. Ideally, the geolocation quality flag should be used to remove bad and suspect pixels with a value of 4 or more, but that leaves too few pixels (in many cases none) for performing a robust analysis. Instead, the threshold for removing pixels was set at a value of 8 or more, which means that pixels with a ”suspect phase unwrapping” are still present in the data. Following Maubant et al. (2025) [25], pixels with a bad interferogram or σ_0 quality and pixels where σ_0 is lower than -36 dB were removed. Following the same approach as for the LakeSP product, the lake outlines from Hows IML inventory were applied to the PIXC data to remove all pixels outside of the lake area. From the remaining valid pixels, the heights were then corrected for the solid earth tide, load tide and pole tide components, to recreate the processing steps of the LakeSP product, but without changing the height reference from the ellipsoid to the geoid. From here, the mean and median water surface elevations could then be calculated along with the standard deviation and mean absolute deviation over all lake pixels for each observation.

For each observation in time a map with all good-quality pixels was created to show which parts of the lake were covered by the pass and which locations experience large deviations or gaps due to bad pixels. This helped provide a better understanding of potential problems influencing the water surface elevation measurements and determine the cause of outliers.

Furthermore, a time series with the mean and median WSE derived from the PIXC product was created including the ICESat-2 derived elevation as WSE reference. Additional data editing based on the

standard deviation and MAD was applied, to remove outliers in the WSE time series. Observations which have a standard deviation of >20 m or an MAD of >10 m were removed, because they both indicate that the WSE estimate will be unreliable. Single outliers were combatted by removing pixels that deviate from the previous and following observation by more than 10 m. These thresholds were set through trial and error and should be considered as a trade-off between the amount of data that is left and the accuracy of the results. The layover error was not used as a criterion here, because it could already be taken into account when removing individual pixels. Comparison of the PIXC and LakeSP time series provided insight on the advantages and limitations of both SWOT data products.

4.5. Error Analysis Based on PIXC

Out of the WSE time series from the LakeSP product, the points which deviate the most are selected as WSE outliers and analysed in more detail with the PIXC product. For this purpose, relevant data variables were chosen from the PIXC data as well as available information from quality flags to perform an error analysis on a pixel-by-pixel basis.

4.5.1. Using the NRCS and Coherence

By visualising the unfiltered pixel cloud over the whole lakes for those outliers, it was possible to spatially locate patterns that indicate causes of WSE errors in the observations. Several relevant attributes in the PIXC product such as the coherent power, the σ_0 and height sensitivities were plotted alongside the water surface elevation to analyse the reasons for errors in the WSE of individual pixels.

The coherent power is an expression of the coherence, which together with the σ_0 are the two fundamental observation characteristics. To find out if water has been detected, the prior water probability (as decimal values from 0 to 1, indicating 0 to 100%) and surface classification, with values described in Table 3.1 were plotted as well. In addition to the layover error and quality flags, parameters which indicate the sensitivity of the height measurements were also included.

4.5.2. Using k-means Clustering

Based on these maps, a visual analysis was conducted comparing single characteristics to the WSE, but not all errors could be identified from looking at individual parameters. That is why the k-means clustering algorithm was employed as a method to detect error causes which are intertwined in multiple parameters and to get an idea which parameters have the largest influence on the WSE.

The principle of k-means clustering is to group a dataset of any number of dimensions into k number of clusters and determine the centroid of each cluster based on the cluster mean value in all dimensions (the whole method is described in section A.1 of the Appendix). There are several methods to determine the optimal number of clusters to use for a given application, but in this application five clusters were chosen for simplicity. The result of the method were five cluster centroids, which group all pixels of one lake observation. Since the centroids were computed for all relevant parameters simultaneously, including the WSE, it was explored how the combination of multiple parameters can influence the WSE. Here the WSE obtained from ICESat-2 was useful to know which centroid lies closest to the true WSE and which centroid has the highest errors.

To take a closer look at the two fundamental observation characteristics, scatter plots between the coherent power, σ_0 and the height were created for the outliers of each lake and compared to the results from the k-means clustering. As part of this, the PIXC outliers were edited to only include open water pixels and compared with the PIXC data where all different water classifications were included. Furthermore, the phase unwrapping and water classification were analysed for example observations, such that errors connected to these aspects can be better understood and avoided.

4.5.3. Naive Approach to Solve Phase Unwrapping Errors

Since phase unwrapping errors are a known problem for lakes and rivers in the SWOT data, NASA has suggested an approximate solution on how to remove a phase unwrapping error without having to repeat the whole phase unwrapping [38]. Instead of adding or subtracting phase ambiguities of 2π to the absolute phase, the geolocation sensitivities with respect to the phase, were added to the latitude, longitude and height, respectively. In this way the location of each pixel was moved with an integer

number of phase ambiguities, towards or away from the satellite, therefore a change in height also results in a change in latitude and longitude. To test how many ambiguities need to be added, different integer values between ± 5 were tested.

4.6. Quality Assessment of the WSE

Finally, all results of the SWOT-derived water surface elevations were compared quantitatively by data product, lake, and different measures of accuracy.

In this study only ICESat-2 measurements were available as reference for the WSE, which did not provide enough observations at a similar time as SWOT observations to be able to perform a real validation of the SWOT data. Thus, the quality of the two SWOT data products for the three chosen IMLs was assessed with three different quantitative measures of accuracy:

1. **WSE variability between pixels**
   First, the height variability of the observed pixel heights was calculated based on the filtered PIXC data. The STD over all pixels of one lake observation was calculated for each observation and then the mean STD was calculated over all observations.
2. **WSE variability between observations**
   Second, from the LakeSP and PIXC products the WSE STD of all observations in time was obtained including all points in the time series of Figure 5.5, 5.8 and 5.11. This variability shows how large the spread of the WSE estimates from different observations is and can give an indication of the internal WSE precision of each SWOT product.
3. **WSE difference between SWOT and ICESat-2**
   As the third measure, the accuracy of the SWOT data was estimated by calculating the difference in WSE between each point and the closest available ICESat-2 measurement in time. This is the closest resemblance to a measure of the SWOT accuracy and the best way to take the temporal variation into account in the absence of gauge measurements.

4.7. Utilising the DelftBlue High Performance Computing system

For efficient processing of the large SWOT data volumes, especially over longer time scales, the DelftBlue High Performance Computing (HPC) system was utilised. By uploading the chosen SWOT data and a Python- and batch script with the processing code, DelftBlue could produce the results in minutes, which would otherwise have taken hours on a normal laptop. This is because HPC systems are not only powerful computers with many Core Processing Units (CPUs), but they are also ideal for processing tasks in parallel. As part of this project, parallel processing was implemented to process several SWOT data files in parallel, reducing the runtime significantly and leading to a more scalable processing method. In this project, 3 parallel tasks were run with 8 CPUs each, therefore a time limit of 20 min was enough in most cases. The parallel processing approach is very useful for upscaling the processing of large amounts of satellite data such as analysing many lakes simultaneously.

5

Results

First, the observations based on the analysis of SWOT data across the whole southwest basin of Greenland are presented in this chapter followed by the main results for each of the three chosen lakes. Finally, the outcome of the error investigation is presented together with the analysis of outliers.

5.1. General Observations from the LakeSP Product

In total 515 000 lake features were obtained from the LakeSP product over the period November 2023 to February 2025, distributed over 23 000 recognised lakes. In Figure 5.1 (left) a map of all 535 IMLs which could be extracted from the LakeSP product with the help of How's IML inventory are shown. The yellow circles indicate the location of the three lakes of interest. The other map (right) shows one dot for each IML with more than 7 observations, with the size of the dot indicating the lake area observed by SWOT, and the colour indicating the number of SWOT overpasses in which each lake is recognised via their lake id. These maps show that a large amount of IMLs in all sizes are present along the whole southwestern border of the Greenland ice sheet, and that most larger lakes seem to have a high number of observations.

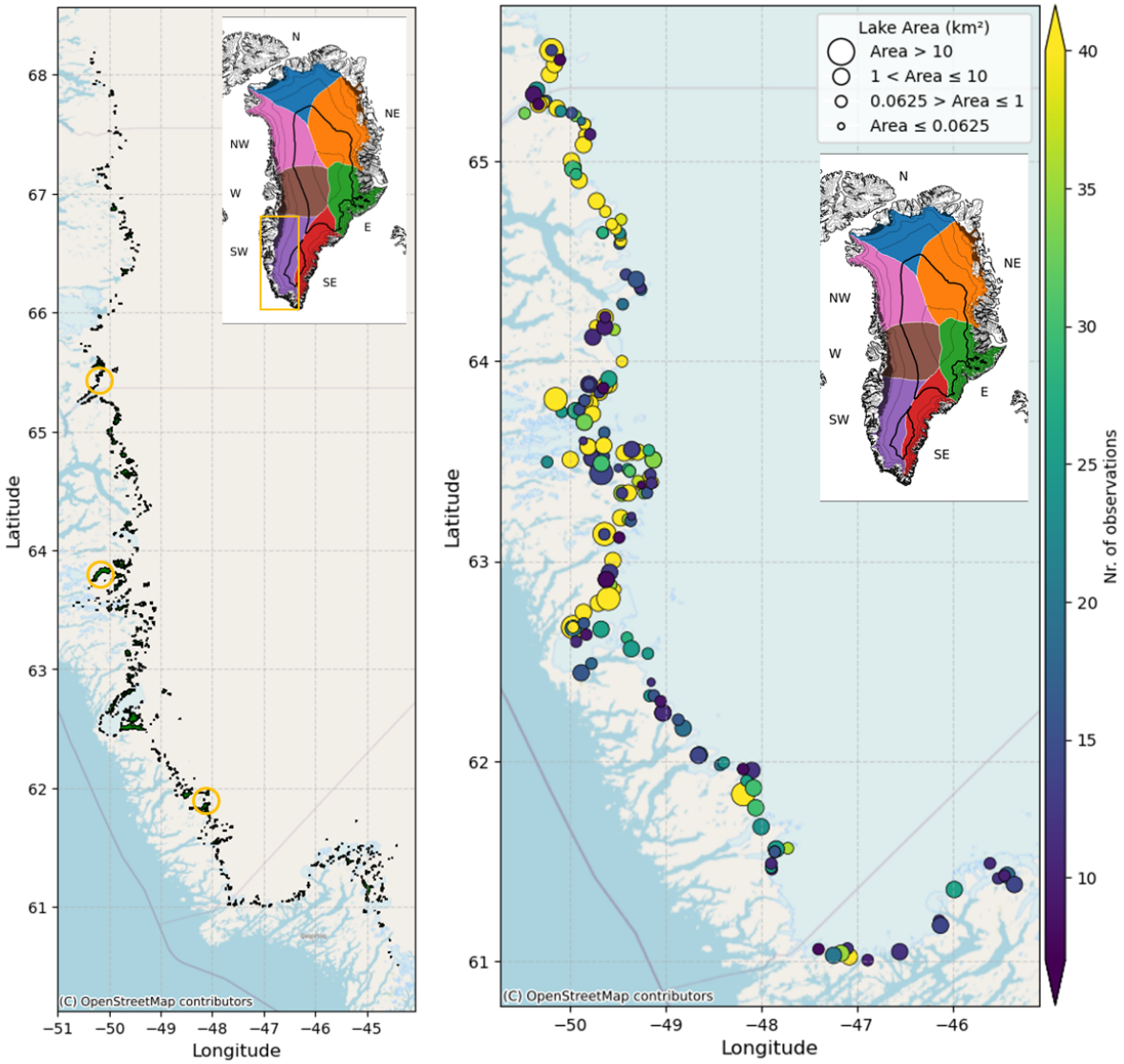

Figure 5.1: Map of all ice marginal lakes observed by SWOT in southwest Greenland (left). In the center of the yellow circles are the locations of the three chosen lakes. The map on the right shows how many observations are available for each lake and they are categorised by lake area. The minimaps show the location of the analysed region as one of seven drainage basins from Brils et al. [5].

From Figure 5.2 (a) it can be seen that many of the lake geometries observed by SWOT (green and red) are affected by specular ringing, indicated by unrealistic lake outlines and stripes going out from the lakes. The IMLs detected via Dømgaards dataset (red in Figure 5.2 (a)) show many lake outlines which are affected by specular ringing, while IMLs detected with Hows dataset (green in (b)) show a lot of smaller lake areas than the observed lake areas in (a). It can also be compared from Figure 5.2 (b) how well the two datasets of IMLs align, and it seems that How captures more small lakes than Dømgaard, which is an advantage.

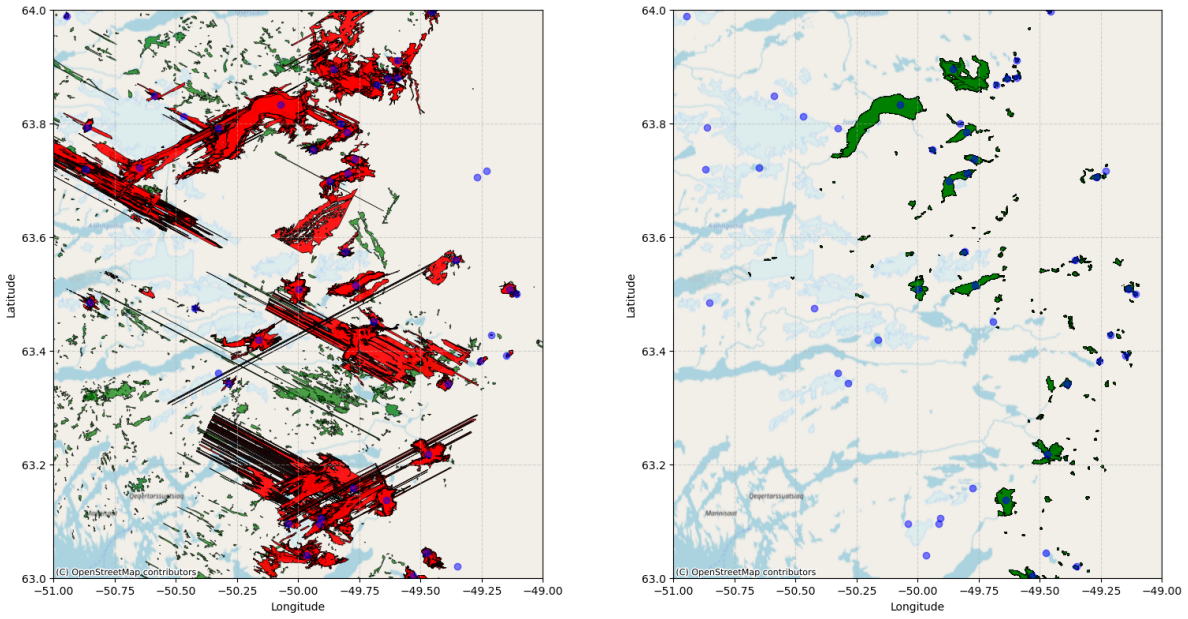

(a) (b)

Figure 5.2: Zoomed-in map of a) all lakes recorded in the LakeSP product (green), IMLs in Dømgaards dataset (blue dots) and lakes which were observed by SWOT and intersect with IMLs from Dømgaards dataset (red) b) observed IMLs by SWOT which intersect IMLs from Hows dataset (green) and IMLs in Dømgaards dataset. (blue dots). Comparing the red lakes in a) and the green lakes in b) shows the discrepancies between the SWOT-observed IMLs obtained with Dømgaards and Hows datasets.

5.2. Time Series of WSE from SWOT and ICESat-2

For the three chosen lakes, the water surface elevations found from both SWOT products are presented in time series with ICESat-2 as reference both before and after outlier removal.

5.2.1. Lake Isortuarsuup Tasia

Results from LakeSP and ICESat-2

Based on the quality flagging criteria described in subsection 4.1.2, the WSE time series of all LakeSP observations for lake Isortuarsuup Tasia is shown in Figure 5.3 including quality flag indicators of affected values. The black line and points around 492 m show the water surface elevation obtained from

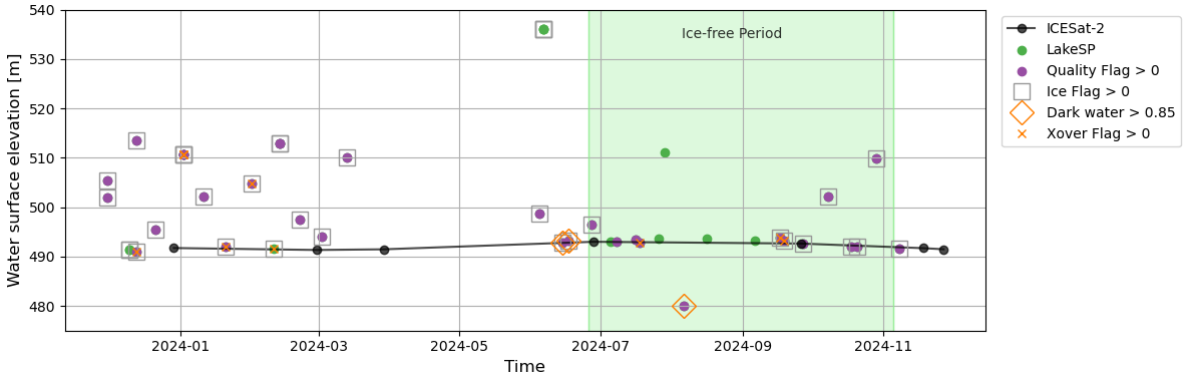

Figure 5.3: Time series of the water surface elevation with respect to the WGS84 ellipsoid at lake Isortuarsuup Tasia as recorded in the SWOT LakeSP product (green and purple points) and by ICESat-2 (black points) for reference.

ICESat-2 as reference for the ”true” water level in the absence of in-situ measurements. Most of the points are purple, showing that the overall quality of these observations is deemed suspect or bad, while only a few of the points are green, meaning they have a good overall quality. In the ice free period, several points are green and have no quality flag markings, while the ice covered period con-

tains almost exclusively purple points, indicating a lower data quality. There is also a clear difference in the WSE variability, because the majority of points in the ice-free period intersects the black line from ICESat-2, which is not the case during the ice-covered period. Even though the time series only spans one year, there are 36 observations of this lake, meaning an average of 3 valid observations per month. However, the observations are not uniformly distributed, since a large data gap is present from March to June 2024. Upon further investigation, it was discovered that the reason for this is, that the lake recognition algorithm which assigns the lake ids failed, so that no lake ids were assigned to any lakes in the pixel cloud. Since the LakeSP product depends on lake id's to know which feature is observed, these observations could not be included in the product. However, they are present in the PIXC product.

As can be seen from the y-axis scale, some observations deviate from the ICESat-2 water level by more than 10 m, resulting in a large MAD of 19.5 m. This voices the need for further data editing, described in section 4.3.

Results from PIXC and ICESat-2

The time series of water surface elevations derived from the PIXC product over lake Isortuarsuup Tasia can be seen on figure Figure 5.4 with both the median (green) and mean (orange) WSE of each observation. Additionally, the median and mean WSE is also shown including bad pixels in a more opaque colour.

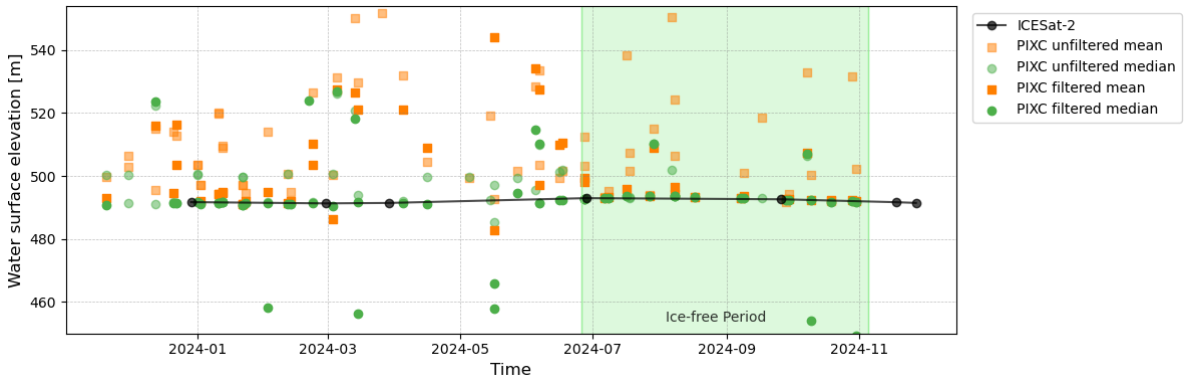

Figure 5.4: Time series of the water surface elevation at lake Isortuarsuup Tasia derived from the SWOT PIXC product median (green) and mean (orange) with ICESat-2 (black) for reference. Here it is shown how the values change when quality flag filtering is applied.

From this result it was observed that the SWOT-derived mean WSE is often overestimated and that the WSE variability of the edited data is smaller. Even though the edited data still have several outliers in the order of meters, in most cases the mean and median WSE of the edited data lie closer to the ICESat-2 observations. Particularly, the median values are in close proximity to the ICESat-2 observations, while the mean tends to overestimate the WSE.

Comparison of the Two SWOT Products

In Figure 5.5 both the LakeSP- and PIXC-derived WSE were plotted for comparison, after removing outliers based on the criteria described in chapter 4, but only the median WSE was included for the PIXC product.

Both SWOT data products seem to have captured a yearly cycle in water level, which is also present in the ICESat-2 data. The observed cyclical variation in WSE can likely be attributed to meltwater runoff from the margin glacier and surrounding mountains, increasing the lake storage in spring and summer, when the snow and glacier experienced melting, followed by a slow decrease in water level in autumn and winter when the lake returned to its equilibrium water level. While both datasets experienced gaps in the ice-covered period, the PIXC product managed to produce more observations with valid data than the LakeSP product, because it could capture lake pixels even when the lake itself was not recognised through the lake id.

In the ice-free period, where the SWOT-derived WSE is most consistent in time, there seems to be a

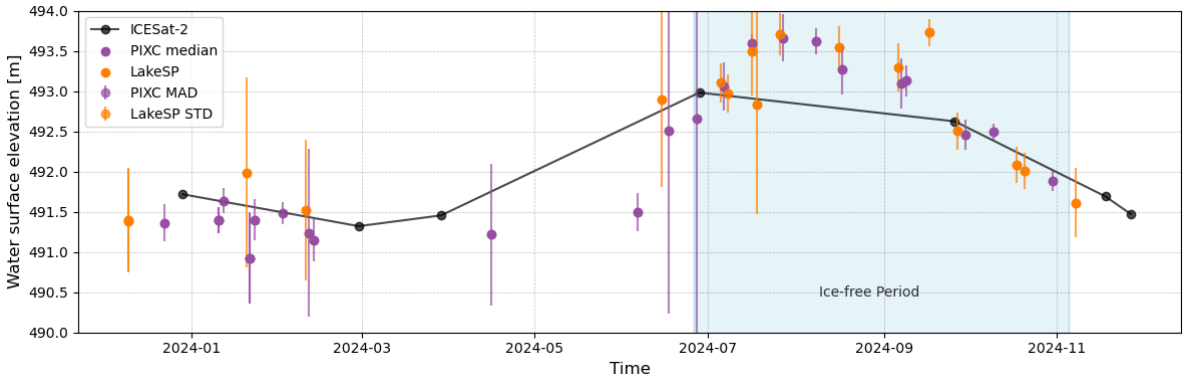

Figure 5.5: Time series of the water surface elevation at lake Isortuarsuup Tasia after removing WSE outliers from the SWOT LakeSP (orange) and PIXC product (purple) based on the STD and MAD of each point. ICESat-2 observed elevations (black) are given as reference.

peak in water level, which is higher than what is observed by ICESat-2. However, this peak cannot be disregarded as an error in water level, because the ICESat-2 observations are too sparse to know whether the true water level indeed increased to this amount. This difference in temporal coverage, and the fact that ICESat-2 itself is a satellite altimeter with a certain accuracy, means that we cannot compute an error estimate between SWOT and the true water level at the time of observation. Overall, the SWOT-derived WSE on lake Isortuarsuup Tasia after data editing was able to capture annual variability in greater detail than ICESat-2.

5.2.2. Small Lake

Results from LakeSP and ICESat-2

The WSE time series of the small lake obtained from the LakeSP product is shown in Figure 5.6 including quality flagging and ICESat-2 as a reference WSE. A notable difference with respect to the lake Isortuarsuup Tasia is that the small lake has much fewer observations (both from SWOT and ICESat-2) than the lake Isortuarsuup Tasia and therefore also has fewer outliers and a much smaller MAD of 0.37 m. Almost no observations outside of the short ice-free period were available, but the observations in the ice-free period seem to be in good agreement with the reference elevation from ICESat-2.

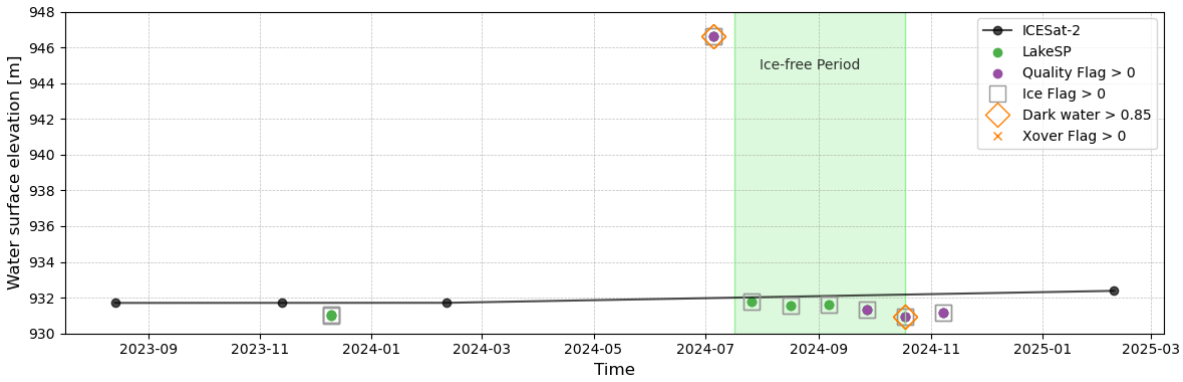

Figure 5.6: WSE time series of the SWOT LakeSP observations (green and purple), and ICESat-2 observations (black) of the small lake.

Results from PIXC and ICESat-2

For the small lake, the number of observations from the PIXC product (Figure 5.7) is significantly higher in the ice-covered period, and many of the observations provide a good WSE estimate when compared to ICESat-2 observations. These water surface elevations were obtained from PIXC after removing bad-quality pixels, similar as done for the lake Isortuarsuup Tasia. In this case it can be seen, that the median WSE does not provide better estimates than the mean.

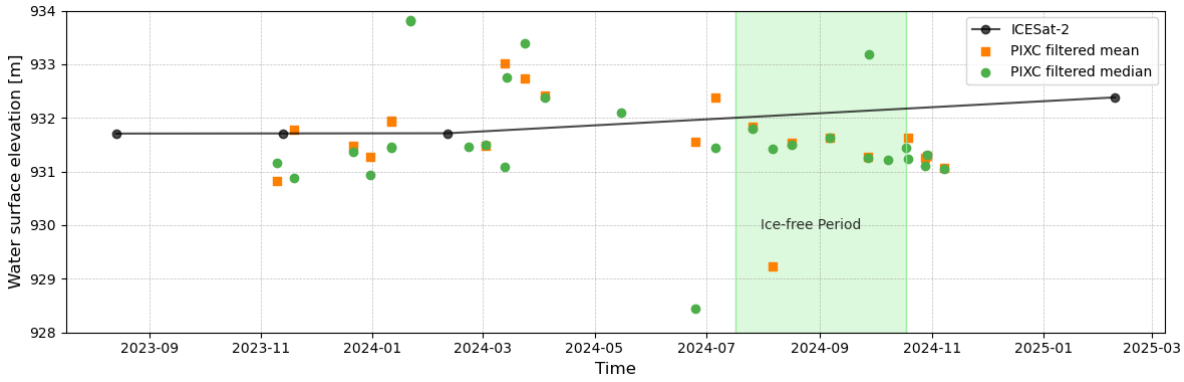

Figure 5.7: Time series of the small lake with the PIXC-derived median (green) and mean (orange) WSE after removing ”bad pixels” based on quality flags, including ICESat-2 elevations (black) for reference.

Comparison of the Two SWOT Products

The WSEs obtained from the two SWOT data products are shown together with their uncertainties in Figure 5.8 after filtering out outliers based on the STD and MAD as before. The problem of ice cover becomes apparent, since observations in the ice-covered period have a much larger uncertainty (STD or MAD) than the observations in the ice-free period. However, all of these observations are within 1 m of the ICESat-2 mean WSE.

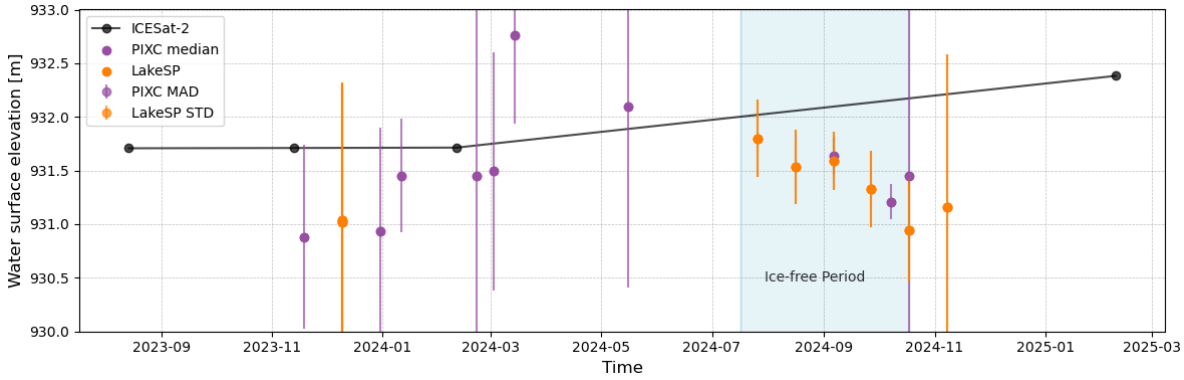

Figure 5.8: WSE time series of the small lake after removing WSE outliers from the SWOT LakeSP (orange) and PIXC product (purple). The STD of the LakeSP points and MAD of PIXC points are shown as error bars. ICESat-2 observed elevations (black) are shown as reference.

5.2.3. Medium-sized Lake

Results from LakeSP and ICESat-2

As can be seen in Figure 5.9 the water surface elevation is around 673 m above the reference ellipsoid according to ICESat-2. The points in green and purple in Figure 5.9 show the derived WSE mean from the LakeSP product together with an indication of quality for the four main quality flags in the product. It should be noted that the scale on the y-axis spans a broad height range due to outliers. Thus, the MAD over these SWOT observations is 3.09 m.

Results from PIXC and ICESat-2

The WSE derived from the PIXC product in Figure 5.10 shows, that the median lies closer to the reference WSE than the mean in most cases, such as for the lake Isortuarsuup Tasia. Although these WSE estimates were calculated from the good-quality pixels in the lake observations, they still have a large variability.

Comparison of the Two SWOT Products

The results from the LakeSP and PIXC product after removing outliers of the WSE are shown in Figure 5.11 in orange and purple, respectively, together with the ICESat-2 estimated height in black for

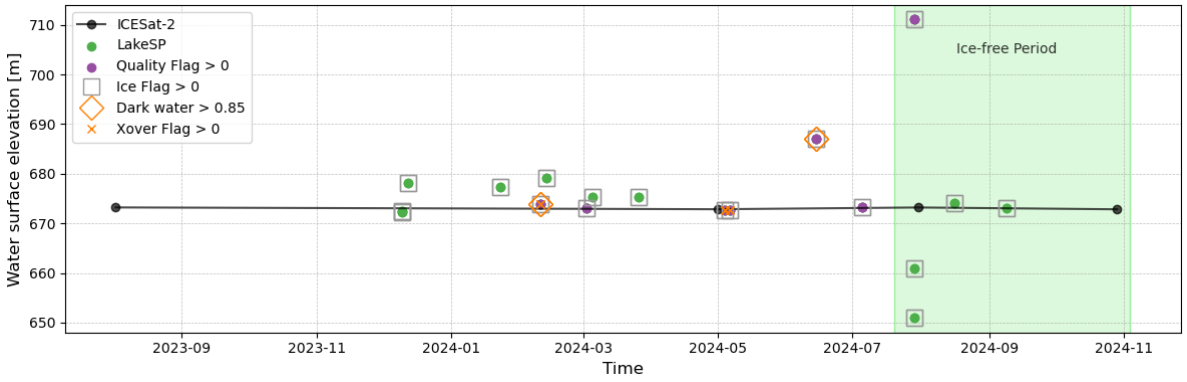

Figure 5.9: WSE from the LakeSP product of the medium-sized lake for good quality (green) and bad quality observations (purple) compared to ICESat-2 (black). The other markers indicate whether specific quality flag issues are encountered.

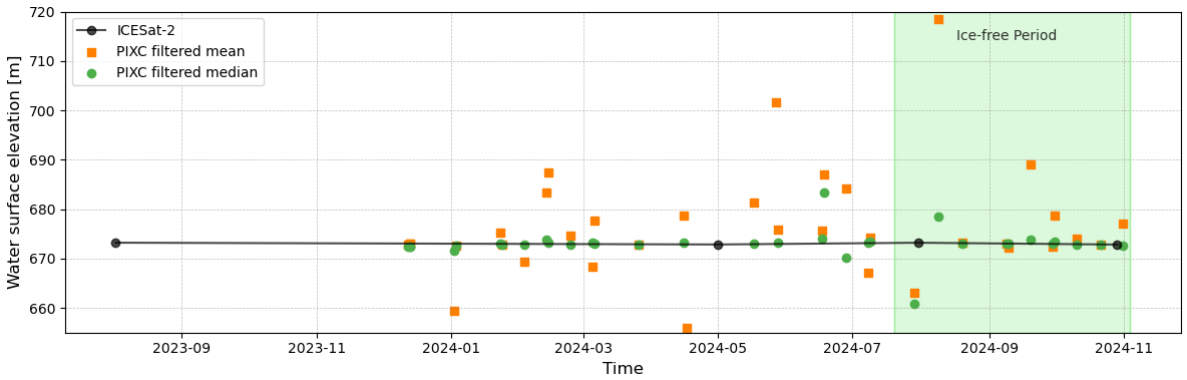

Figure 5.10: WSE from the PIXC product of the medium-sized lake based on the mean WSE (orange) and median WSE (green) for each observation compared to ICESat-2 (black).

reference. Since one outlier is still present after filtering, the scale is coarser than for the other two

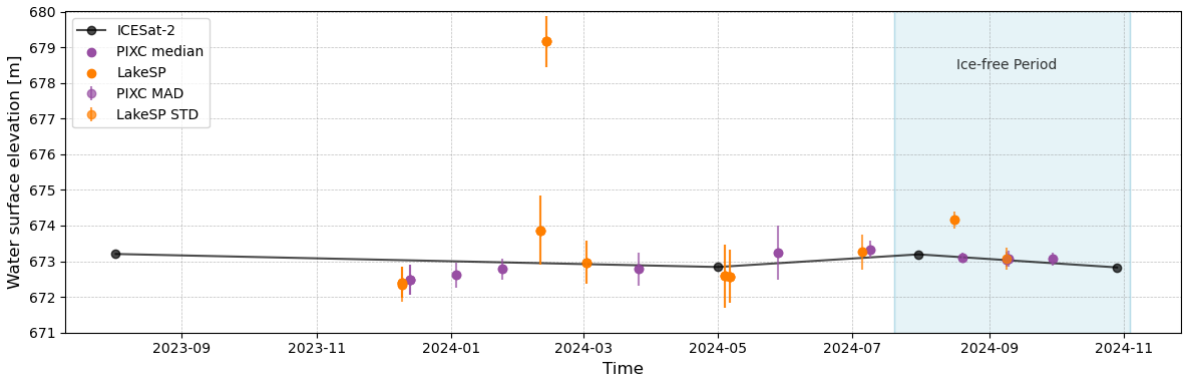

Figure 5.11: Time series of the WSE at the medium-sized lake after removing WSE outliers from the SWOT LakeSP (orange) and PIXC product (purple) based on the STD and MAD for each point. ICESat-2 observed elevation (black) is given as reference.

lakes, but the majority of points are within 1 m from ICESat-2 similarly to the results at the other two lakes. The remaining observations from both SWOT data products are spread out more evenly over the observation period than for the other two lakes, showing that more LakeSP observations were available in the ice-covered period. The ICESat-2 measurements also show a variation in time, indicating that the water level might have a yearly cycle as well, but due to only four observations from one ICESat-2 track being available, it is difficult to tell how much of the variation is truly from the water level and how much stems from measurement uncertainty in ICESat-2.

Collectively, these time series of the three IMLs showed that the median WSE is the preferred choice for retrieving the most accurate WSE from the PIXC data to reduce the influence from pixel outliers which are common for IMLs. Since the ice-free period is small for IMLs in Greenland, the observations obtained by the PIXC product are valuable for providing information during the ice-covered period because the LakeSP product often provides very few WSE estimates in that period. However, both products experience high uncertainties during the ice-covered period, meaning these observations are not very reliable. The small lake showed that reasonable WSE estimates can be derived from SWOT for IMLs with an area as small as 0.2 km^2.

5.3. Results from LakeSP Error Analysis

The error analysis based on the LakeSP dataset of all observed IMLs in southwest Greenland, is shown here to understand where the uncertainty in the LakeSP product comes from and if any patterns are present when observing IMLs with SWOT.

From the histogram of MADs for each observed IML in Figure 5.12 it can be seen that many lakes have a small MAD <1 m, but a MAD of <5 m is not uncommon either. This suggests that many ice marginal lakes in Greenland have significantly larger WSE variations between LakeSP observations than would be expected, except if a GLOF event occurred. The x-axis was cut off at 20 m to show the distribution in better detail, because only very few lakes possessed a MAD above 20 m. Such a high uncertainty can be the result of several factors, which is why the correlations between several chosen parameters and the MAD are shown in Figure 5.13 together with the Pearson correlation coefficient r. Each dot

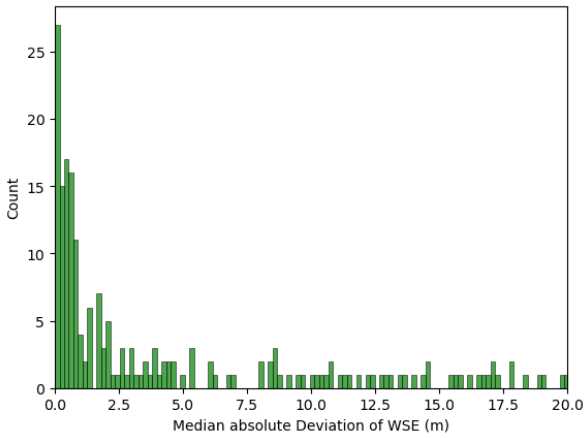

Figure 5.12: Histogram of the MADs calculated for each SWOT observed IML in the LakeSP product. Each lake produces one MAD calculated across all observations of that lake in time, therefore the MAD shows the WSE uncertainty of each lake as observed by SWOT.

corresponds to one IML, for which the average value of each parameter over the whole observation period is shown. There seems to be no indication that the size or location of the lake with respect to the satellite has any correlation with the MAD, and neither do any of the quality flags. It should be noted that the average layover errors of the lakes have an order of magnitude of $10^{-3} - 10^{0}$ m, meaning that many IMLs in the LakeSP product have errors up to several decimeters in the water surface elevation. The parameter with the highest Pearson correlation coefficient is the number of observations ($r = 0.46$), indicating that more observations of a lake result in a higher MAD. However, this r value is still quite low and therefore should not be given too much significance. In Appendix A, Figure A.4 one of the time series with a very large MAD and many observations is shown, where the large WSE differences and multiple WSE estimates from the same date indicate that multiple lakes have been observed and classified into one lake-id.

To conclude, it was not possible to find the error causes in the LakeSP product by only analysing the LakeSP product itself through the MAD. In order to understand the causes of the high MADs, the PIXC product was utilised for a more detailed error analysis.

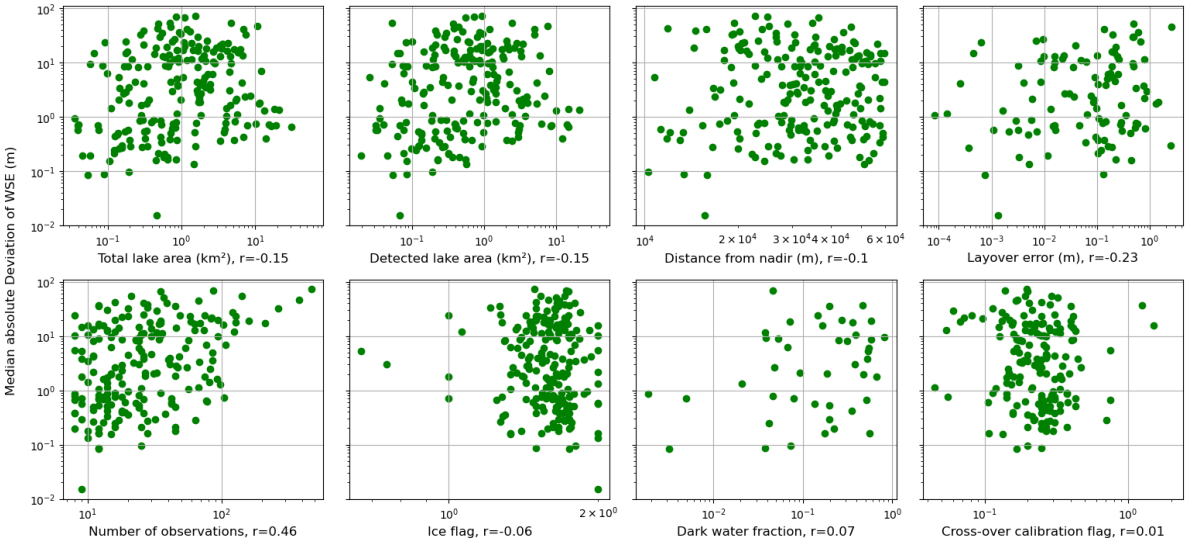

Figure 5.13: Pearson correlation coefficient r and scatter plots between LakeSP MAD and different parameters from the LakeSP product. Each dot represents one IML.

5.4. Results from PIXC Error Analysis

For several outliers present in the WSE time series of each lake, the analysis of the PIXC data is shown here. An overview of all analysed parameters can be seen in Appendix A, Figure A.5, Figure A.6 and Figure A.7. On Figure 5.14 a SWOT observation from the 17.09.2024 of lake Isortuarsuup Tasia can be seen. At locations where the coherence and σ_0 are high (upper right of the lake), the height is closer

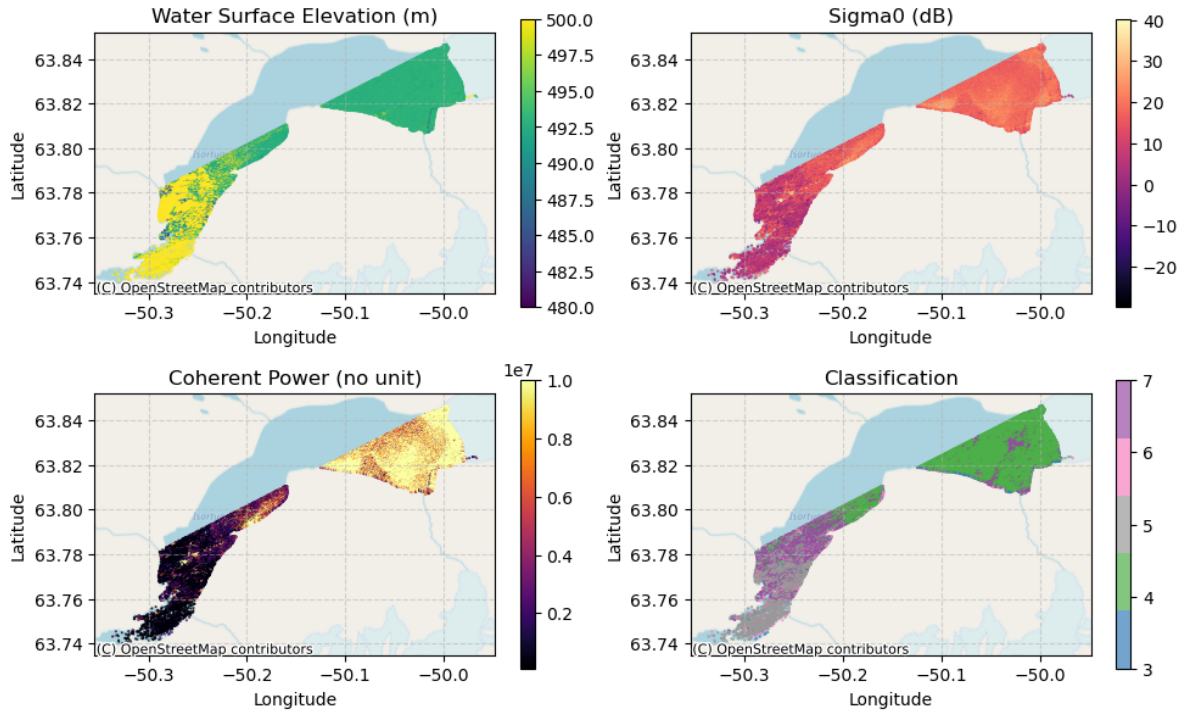

Figure 5.14: Pixel cloud data of Isortuarsuup Tasia from an observation on the 17.09.2024 showing the WSE, σ_0, coherent power and classification of each pixel.

to the ICESat-2 measured WSE around 492 m, but at locations where they are low, the heights deviate more and a higher variability between pixels is observed. This indicates that the σ_0 and the coherence have a strong influence on the estimated height, which is true for most of the observations. These

two parameters in turn influence the classification, where it is observed that pixels with high σ_0 and high coherence are classified as 'open water', while pixels with low coherence and σ_0 are more often classified as 'dark water' or 'low coherence water'.

5.4.1. Using the NRCS and Coherence

An example of how important the NRCS (σ_0) and coherence are, is lake Hullet. It is present in the LakeSP product as well as the PIXC product with its own lake id, but the observed water levels are consistently more than 100 m higher than the ICESat-2 reference and other sources such as the Danish Agency for Data Supply and Information [11]. As can be seen in Figure 5.15, the area where lake Hullet (outlined in black) should be, is only observed with a low σ_0 (left) and a low coherence (right), while other water bodies are bright due to a high σ_0 and high coherence. This means that the lake could not really be detected and is only classified as 'dark water' because the Prior Lake Database determined that the lake should be present at that location.

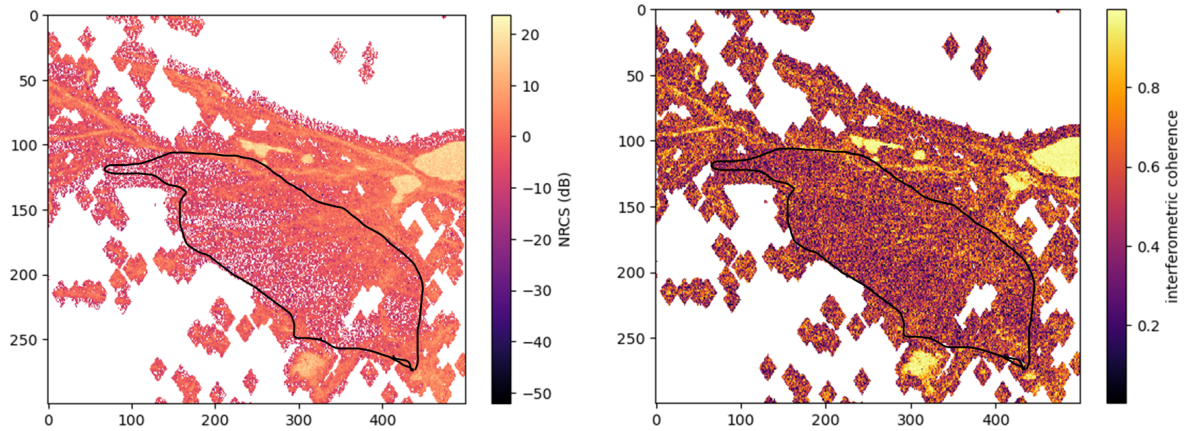

Figure 5.15: NRCS (σ_0) (left) and interferometric coherence (right) show that lake Hullet (outlined in black) is not detected by SWOT because it has a low backscatter and low coherence. The pixels are shown in the radar coordinates with range distance (m) on the x-axis and azimuth distance (m) on the y-axis. The plots only contain pixels classified as water.

By plotting the σ_0 and coherence against the height for the above mentioned outlier of the lake Isortuarsuup Tasia (see Figure 5.16), it was confirmed that both parameters show a spike of high coherence/σ_0 around 492 m, where the real WSE should be according to ICESat-2. However, the spike is not always

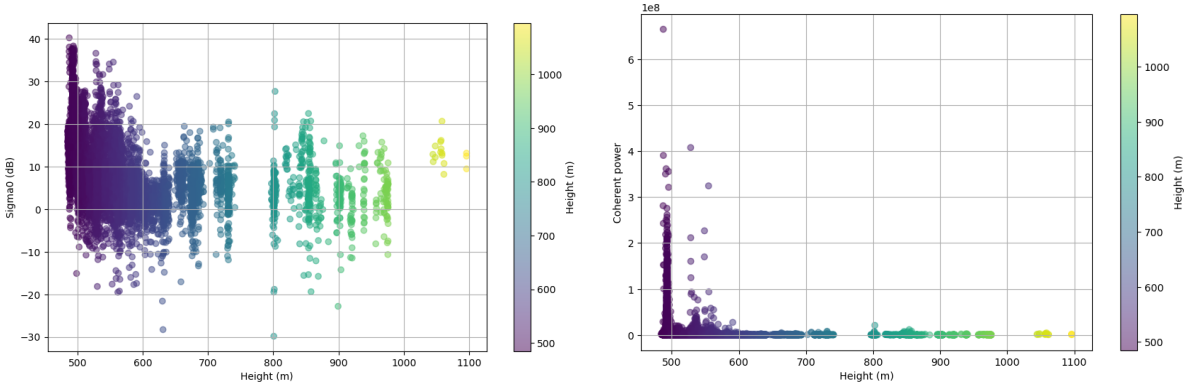

Figure 5.16: The NRCS (σ_0) (left) and coherent power (right) for the PIXC product of lake Isortuarsuup Tasia on the 17.09.2024 show a peak around 492 m height, which is in agreement with the expected WSE according to ICESat-2.

as clear as the coherence shows in this figure, and it is also important to know what the connection between these two parameters is.

In Figure 5.17, where the σ_0 is plotted against the coherence, the relationship becomes clearer. When both parameters are plotted on a logarithmic scale, a linear relationship is observed, meaning that for

increasing σ_0, the coherent power also increases, except at the lower left end. The pixels with the highest σ_0 and coherence are mostly blue, so their height lies close to the true WSE of 492 m, while pixels with low values of both parameters give height estimates that show much larger discrepancies.

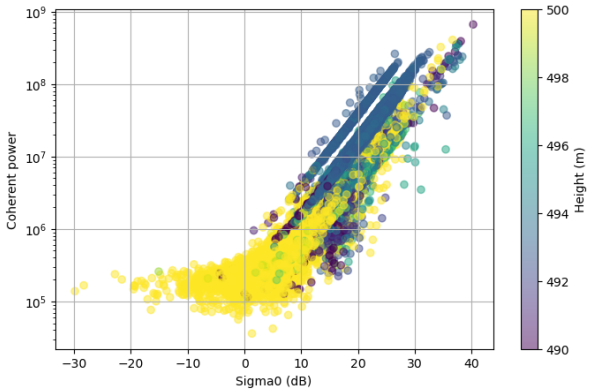

Figure 5.17: Pixel cloud data of lake Isortuarsuup Tasia from the outlier on the 17.09.2024 showing the linear relationship between the σ_0 and coherent power, with the WSE of each pixel indicated in colour. The ICESat-2 measured height is around 492 m.

5.4.2. Using k-means Clustering

After applying k-means clustering to an observation of the medium-sized lake, including the height, height to phase sensitivity, coherence, layover error and σ_0 among others, the five centroids shown in Table 5.1 were obtained.

Table 5.1: k-means clustering result of a medium-sized lake observation from the 09.07.2024 calculated with 5 cluster centroids and 5 of the PIXC parameters.

Height (m)	dHeight/dPhase (m/rad)	Coherence (-)	Layover error (m)	σ_0 (dB)
675.98	7.03	7.57e+05	0.082	-1.77
673.48	7.19	2.33e+07	0.33	16.57
674.20	7.18	9.90e+06	0.15	12.91
673.56	**7.17**	**2.17e+08**	**0.36**	**26.36**
673.37	7.19	4.66e+07	0.41	19.25

The centroid with the lowest coherence and lowest σ_0 also has the worst height estimate, while the opposite is the case for the centroid marked in bold. Similar to the visual analysis, the strongest connection was observed between the values of height (WSE), coherence and σ_0, followed by a weaker connection to the height to phase sensitivity and layover error, while the values of other parameters showed no clear patterns related to the height values of each centroid. Unfortunately, from the centroid results of other outliers it was concluded that the k-means clustering method does not always find centroids with good WSE estimates. Several of the outliers encountered additional problems, which could not be resolved by k-means clustering alone.

Two of these problematic outliers are shown in Figure 5.18 of the medium-sized lake on the 13.02.2024 (left) and the small lake on the 21.02.2024 (right). On these scatter plots the true water level is not distinguishable from the pixel cloud.

This medium-sized lake outlier does not show the expected WSE for pixels with high σ_0 and coherence, or through k-means clustering, which should be around 673 m. Also in this case, most of the pixels were classified as dark water. Only by using exclusively bright and open water pixels a realistic WSE estimate of 674.6 m could be achieved from the median, which is still approximately 1 m too high. If the scatter-plot is recreated with only open water pixels (see Figure 5.19), it can be seen that they all have a high σ_0 and high coherence as they should. Even so, there are many open water pixels with large deviating height estimates.

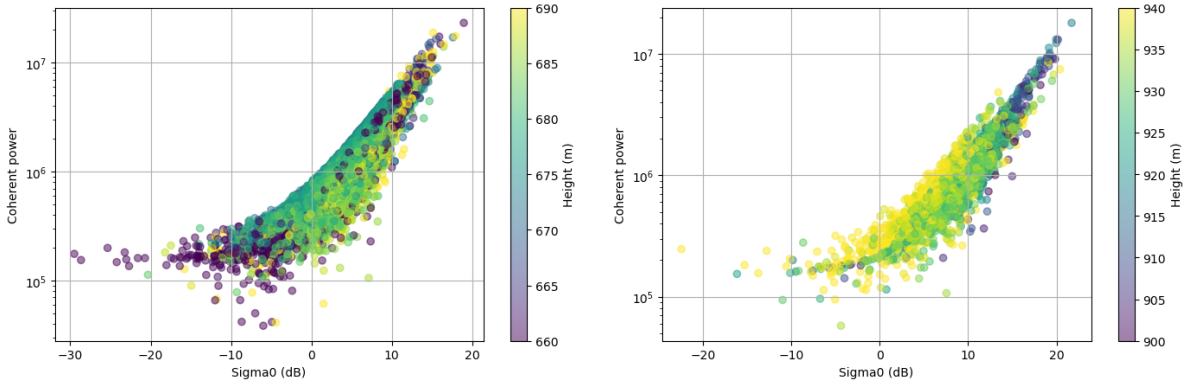

Figure 5.18: Scatter plots of the σ_0 against the coherence including the height in colour of two outliers from the medium and small lake, respectively.

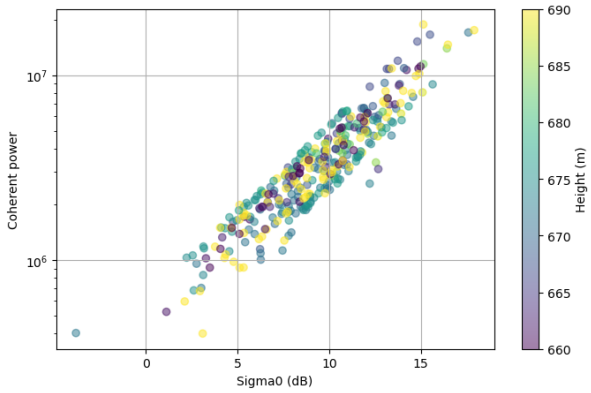

Figure 5.19: Observation of the medium-sized lake from the 13.02.2024 only including open water pixels. All pixels have high coherence and σ_0 but have a large water level variability.

When looking at the small lake outlier in Figure 5.18, determining the error causes becomes more complicated. In Figure 5.20 the water surface elevation is shown next to the σ_0, coherence and classification. Here it can be seen that the areas with high σ_0 and coherence have a much lower water level than ICESat-2, which measured a WSE around 931 m. Also, these areas were classified as low coherence water and it seems like an error occurred in geolocating the pixels, because the right side of the lake is not covered.

k-means clustering showed that the centroid with the highest coherence and σ_0, which should include the best quality of observations, resulted in a WSE estimate of 913 m, a lot lower than the expected WSE of 931 m. Still, the obtained median WSE for all pixels of 931.88 m lies close to the ICESat-2 reference. Through analysis of the individual classes (see Table 5.2), it was observed that open water pixels (class 4) alone resulted in an underestimation of the height estimate. Even though the other classes have very wrong height estimates, they manage to counterbalance the underestimation of the surface height from class 4, which can be noticed in the high MAD and STD of this observation.

To illustrate how much data is available if only open water pixels would be used to calculate the WSE, all open water pixels from an observation of the large, medium and small lake are shown in Figure 5.21. As could be expected, the small and medium-sized lakes were affected significantly more, since some observations of the small lake already contained less than 10 points including dark water pixels, or only consisted of dark water pixels such as lake Hullet. Larger lakes such as lake Isortuarsuup Tasia were less affected by a loss of observations, because they are observed more often and contain more pixels per observation. However, this observation of the lake Isortuarsuup Tasia also shows that pixels can be wrongly classified as open water and posses large WSE variations, because Sentinel-2 images showed that the lake was fully ice covered at the time of observation. This is another reason for the data gap in the time series of the lake Isortuarsuup Tasia, where this observation was not included.

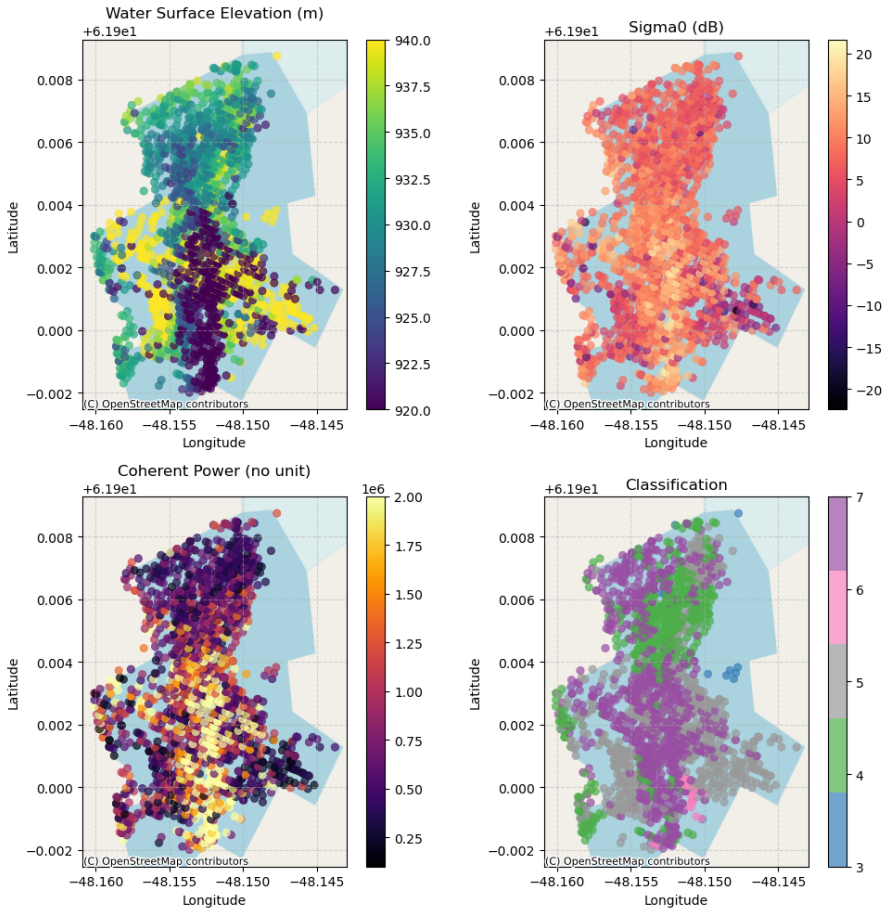

Figure 5.20: Small lake Outlier from the 21.02.2024 showing the WSE, σ_0, coherence and classification.

Table 5.2: WSE of the small lake derived from the PIXC data from the 21.02.2024. Here the mean and median were calculated for the pixels of each surface class (4=open water, 5=dark water, etc.) separately.

Classification	3	4	5	6	7	Total
mean	994.04	930.01	941.07	934.71	922.98	932.18
median	1033.40	930.80	939.51	936.84	924.52	931.88
std	59.89	4.53	14.37	5.35	10.85	15.24
MAD	56.60	1.69	3.44	1.56	7.12	6.30

5.4.3. Phase Unwrapping Errors

Some of the outliers have also shown signs of phase unwrapping errors, such as the observation of the medium-sized lake from the 02.13.2024 shown on Figure 5.22. Here, a large slope is present in the WSE going perpendicular to the satellite track because it is known that the satellite was located South-East of the lake and looking North-West towards the lake in this observation. From the right map it can be seen that the further away from the satellite a point is, the more sensitive the height calculation becomes to the phase. Therefore, if an error occurred in the phase unwrapping, the height of the lake closer to the satellite was affected differently than the height on the distant side of the lake.

By plotting a cross section of the lake in the range direction away from the satellite (Figure 5.23), it was seen that the height to phase sensitivity is linearly related to the height residual, which was calculated by subtracting the mean ICESat-2 height (673 m) from the PIXC height. This confirmed that a slope in height is an indicator of a phase unwrapping error. When the same parameters were plotted with all lake pixels, the same linear relationship was present but less clear than in the cross-section.

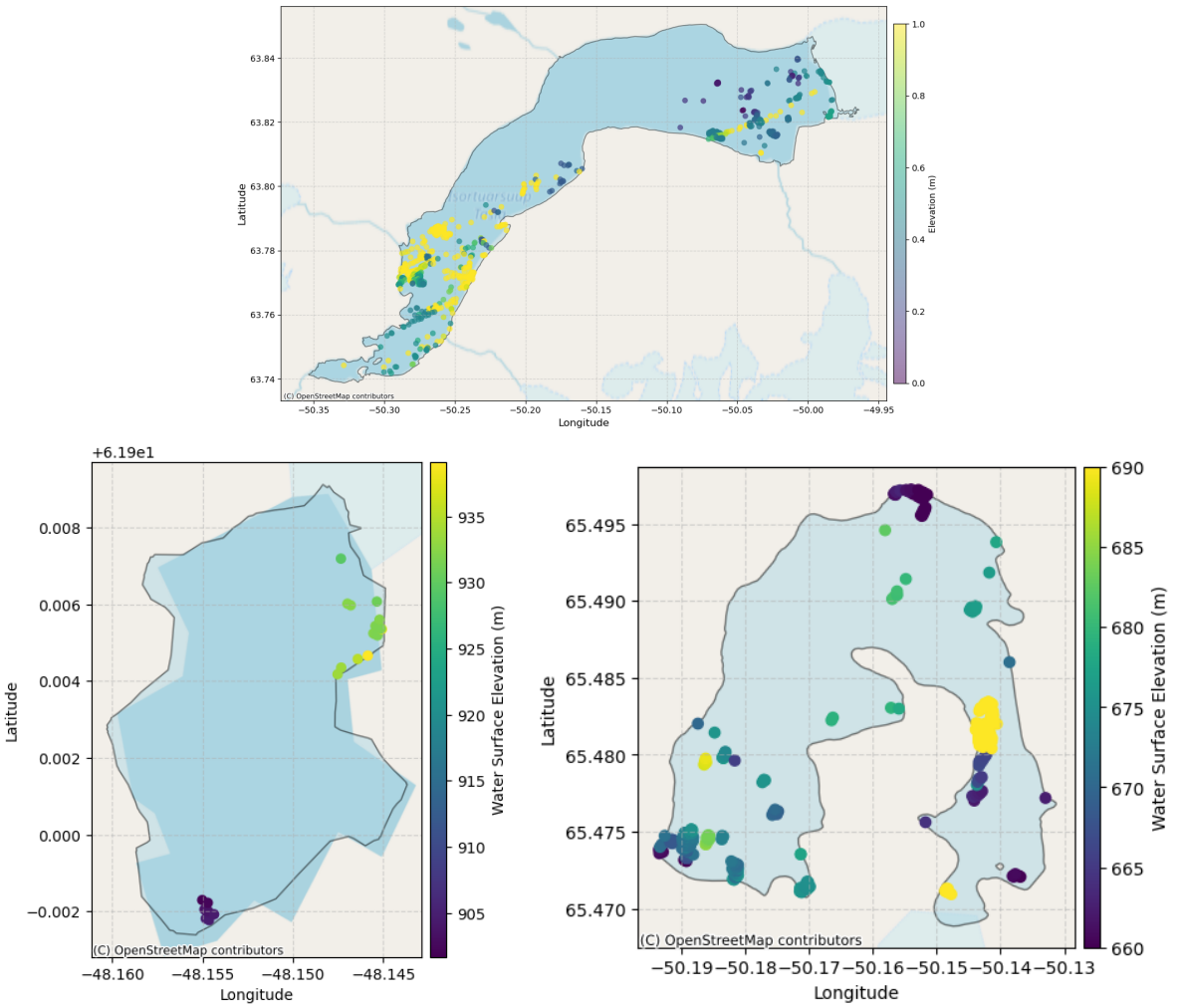

Figure 5.21: Map of only open water pixels for the lake Isortuarsuup Tasia (top), medium-sized lake (bottom left) and small lake (bottom right) from outliers.

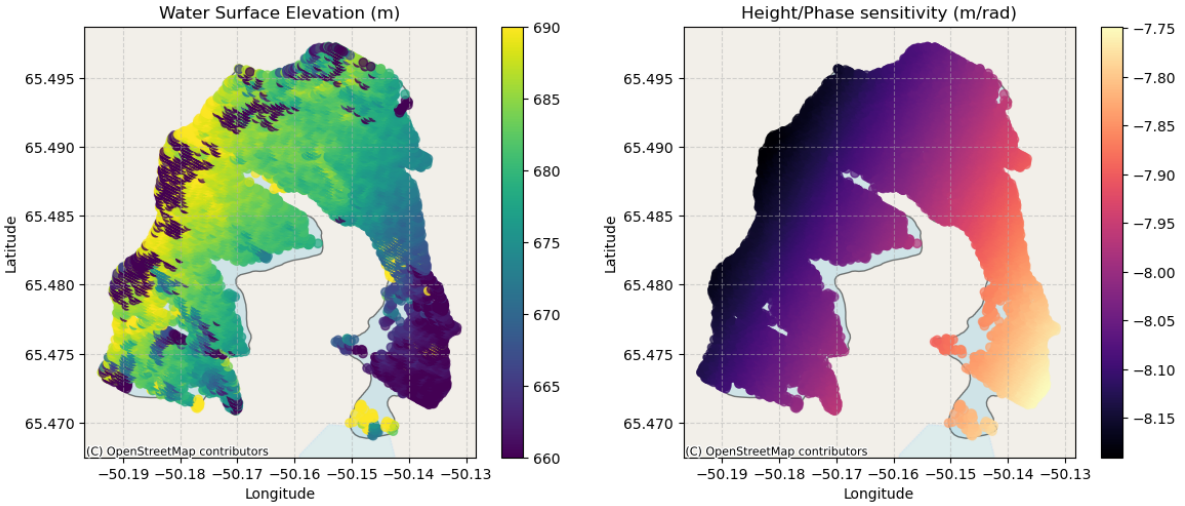

Figure 5.22: WSE of the medium-sized lake outlier from the 02.13.2024 shows a slope in surface height (left) connected to the Height to Phase sensitivity (right) and distance to the satellite.

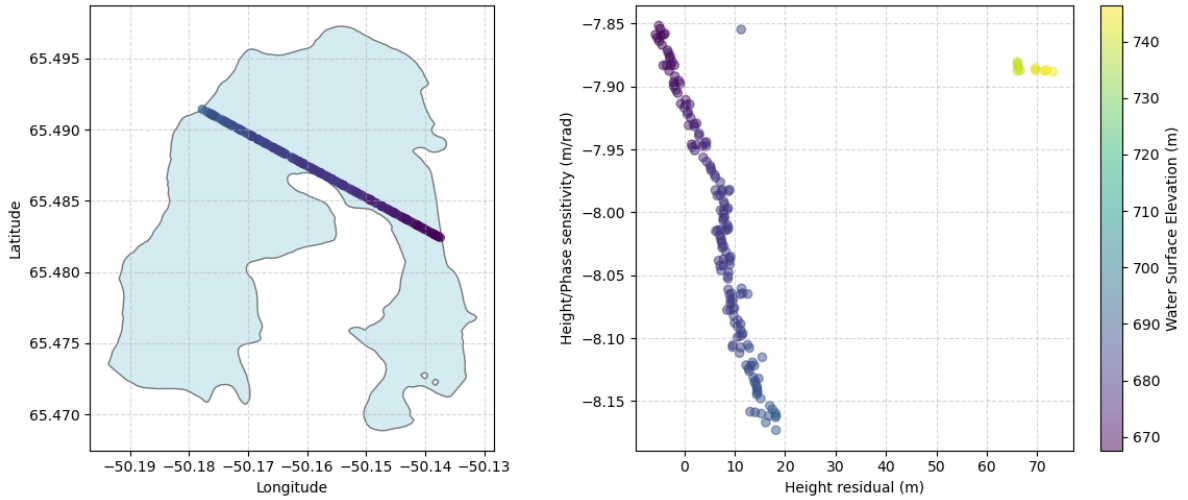

Figure 5.23: Cross-section through the medium-sized lake perpendicular to the satellite track shows slope in water surface elevation (left).

Naive Approach to Solve Phase Unwrapping Errors

In Figure 5.24 the result of the naive approach to solve phase unwrapping errors is shown for $+1$ phase ambiguity. While the height to phase sensitivity over the lake is purely negative, the observed WSE is both higher and lower than the ”true” water level (ICESat-2 mean).

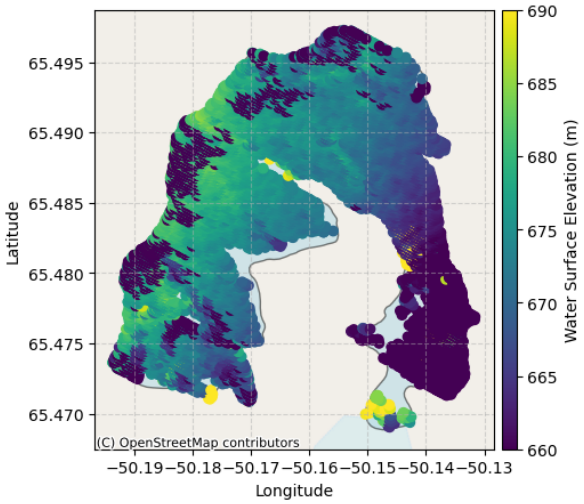

Figure 5.24: Attempt to solve phase unwrapping error by adding one height to phase sensitivity to each pixel. This still results in a large surface elevation slope over the lake, but all elevations are now lower than before.

5.4.4. Dark Water Errors

When looking at a partially ice-covered observation of the medium-sized lake on the 09.07.2024 in Figure 5.25, the ice-covered part is fully classified as dark water, experiences a lot of WSE variability between pixels and produces overall worse WSE estimates. Meanwhile, the area with open water experiences more consistent height measurements that lie closer to the ICESat-2 reference around 673 m.

5.5. Results of Quality Assessment of WSE

The average pixel-to-pixel variability (STD) for the large, small and medium-sized lake are 6.90 m, 7.31 m and 3.58 m respectively. From Table 5.3 it can be seen that the WSE variability between observations

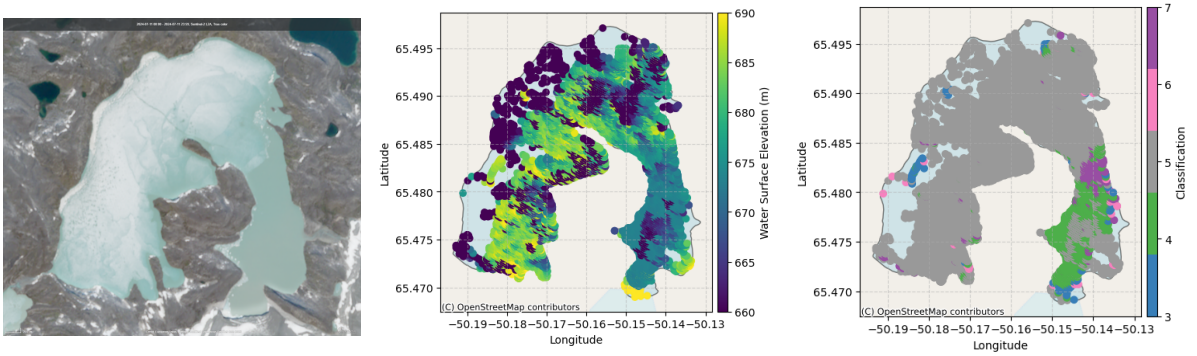

Figure 5.25: Copernicus Sentinel-2 L2A true color image (11.07.2024) processed in Copernicus Browser (left) [1]. SWOT Observation with partial ice cover of the medium-sized lake from the 09.07.2024 (middle and right).

of the LakeSP product is quite high for the large and medium-sized lake and surprisingly low for the small lake. In comparison, the PIXC product has decimeter precision in all three cases. It makes sense that the lake Isortuarsuup Tasia has a higher observation-to-observation variability, because the temporal WSE variation is not taken into account, and a clear WSE variation in time was observed in the order of meters. The medium-sized lake has one large outlier that affects the variability, because the outlier itself has a small STD and MAD, and was therefore not captured during the data editing. Meanwhile, the small lake has less observations and not much temporal change in WSE, leading to a lower variability.

Table 5.3: Comparison of WSE variability between observations for the time series of each lake separated into the observations of each data product. The last two lines show the WSE difference between SWOT observations and the closest ICESat-2 point.

	Isortuarsuup Tasia	**Small Lake**	**medium-sized lake**
PIXC WSE variability (m)	0.90	0.46	0.30
LakeSP WSE variability (m)	4.43	0.30	2.19
PIXC difference to ICESat-2 (m)	0.40	0.55	0.27
LakeSP difference to ICESat-2 (m)	1.38	0.85	1.22

Last but not least, it can be seen from Table 5.3 that the variability for both products with respect to the ICESat-2 WSE is lower than the point-to-point variability in almost all cases. And even though the magnitude of these accuracy estimates is still a lot larger than the mission requirements, most of them are in the decimeter range. From these results it was concluded that the precision and quality of the WSE estimates which can be gained from the PIXC product are significantly better than from the LakeSP product, but users should be aware that this also depends on the applied data editing and number of valid observations. Around 80% of all observations of the lake Isortuarsuup Tasia which were recorded in the PIXC product made it to the LakeSP product, and around 45% of those remained after the strict data editing. Out of the total number of observations, between 26-36% remained in the LakeSP product after data editing for the three lakes analysed here.

6

Discussion and Recommendations

6.1. Discussion

6.1.1. Comparison of SWOT-derived WSE to ICESat-2

The results presented in chapter 5 have shown that the WSE obtained from the PIXC and LakeSP products are subject to variations in the order of several meters from observation to observation. This emphasises the need for extensive data editing in order to retrieve WSE estimates which have a mean deviation of only 0.27 - 1.38 m from the reference WSE measured by ICESat-2. According to a study of rivers and reservoirs in India by Patidar et al. (2025) [27], the 68th percentile of reservoirs achieved a WSE accuracy of 9-14 cm from SWOT observations validated with in-situ measurements from Indias Central Water Commission. Similarly, a study from Australia by Maubant et al. (2025) [25] obtained accuracies of 26 cm for the LakeSP product and around 5 cm for the PIXC product, compared to station gauges provided by the Australian Bureau of Meteorology. Maubant also concluded that some Australian lakes are missing from the PLD, which affects the LakeSP product. Both of these studies were able to achieve WSE accuracies similar or higher than the mission requirements, which was not the case in this study. However, this can be largely attributed to the different conditions (particularly no ice cover) of the lakes in those two studies, and the availability of sub-daily in-situ measurements.

6.1.2. Comparison of Results Between LakeSP and PIXC

While the LakeSP product could be used to obtain WSE timeseries from 535 IMLs in southwest Greenland, the PIXC product provided key insights into error causes such as phase unwrapping, ice cover, and dark water issues. The Median Absolute Deviation across all observations of each lake, which was found from the LakeSP product, showed no strong correlations. This could be because there was too much averaging involved. Since the LakeSP product contains one averaged WSE per lake observation, the MAD could only be calculated across all observations of the given time period. However, parameters such as the dark water classification or layover error are individual from pixel to pixel, as was observed from the PIXC product. The analysis of the PIXC product and k-means clustering were in agreement that the σ_0 and the coherence are the two main indicators for good WSE estimates. These two fundamental parameters also play a role in the determination of lake outlines and pixel classification such as determining dark water pixels.

As was seen in Figure 5.2, many lake observations in the LakeSP product were affected by specular ringing. This significantly impacts the recorded outline and area of the lakes, but also suggests that additional erroneous pixels could be included in the WSE calculation of the LakeSP product. Ideally, the lake outline of each observation could be used to detect if the water level has changed and update the PLD accordingly, but the issues with specular ringing show that the observed lake outlines are far too unreliable for this purpose yet. Therefore, this research resorted to using the lake outlines from How et al. (2021) [24] to make sure that the lake outlines are realistic and avoid impact from specular ringing as far as possible.

Even though the lake surface area was not analysed here, it is apparent that the lake identification

based on the pixels that are present creates unrealistic and highly varying lake outlines in many cases, resulting in bad estimates of lake area and potentially affecting the calculation of the WSE. It should be investigated whether the WSE is affected by checking the `area_wse` variable in the LakeSP product, but the variable is missing from the data files, even though it is mentioned in the documentation. This could give an indication on how realistic the lake area is, over which the WSE is calculated. If the `area_wse` is much larger than the PLD lake area, the WSE estimate might not be very representative. One solution to this is to use PLD lake outlines for retrieving pixels, but then lake extent changes cannot be captured, which also results in errors for the lake surface area and storage change of the LakeSP product.

By comparing the LakeSP and PIXC product of these three lakes, it has been observed that the data points of the two products are often not in the same locations, even though the two products are based on the same satellite observations of the lakes and similar processing. There are two main causes for this, one of them is that some observations are removed in the processing, and are therefore missing from either of the two products. This means that two points lying close together in time from the PIXC and LakeSP product in fact originate from two different satellite overpasses, which can occur with only few days in between. Since the lake Isortuarsuup Tasia is covered by 4 SWOT overpasses, there are 4 potential observations every 21 days, which could be utilised to gain a higher temporal resolution, if the quality of them was better. Combining the two products can take advantage of different processing methods to obtain more valid observations within the given time.

Another reason for different locations is that the processing differs slightly because the data editing of pixels and the derivation of the WSE were adapted for IMLs. Since the uncertainty-weighted mean WSE present in the LakeSP product produces many large outliers, the median was chosen for the PIXC product. Together, these reasons influence the resulting WSE estimates, which is why some PIXC points are located directly above or below the LakeSP points of the same satellite observation.

6.1.3. Determining Main Error Sources

The time series from the LakeSP product with particularly many observations and a high MAD suggested that several lakes have been combined into one lake id. The probable reason is that the lakes could not be distinguished, and therefore the WSE of multiple lakes were mixed together in one time series - leading to a large MAD.

For lake Hullet, the overestimated surface heights most likely occurred due to the lake being categorised into the same phase unwrapping region as the surrounding pixels with low coherence and low σ_0. Since the lake lies in a valley, it is not unlikely that most of the other noisy pixels lie at higher elevations in the mountains, resulting in a higher WSE estimate for lake Hullet as well.

The main issues when looking at the PIXC data from the three chosen lakes were, that many pixels experienced bad geolocations, and many pixels were classified as dark water or low coherence water. Combined, these issues resulted in a very large height variability between different pixels of the same lake observation (3.58 - 7.31 m on average for the three chosen lakes) and thus large uncertainties which propagated to further SWOT data products such as the LakeSP product. For the LakeSP product, this large variability was overcome by using a height-constrained geolocation, but using an average WSE also removed the ability to spatially distinguish any patterns from the height. Since the geolocation is closely connected with the height estimate, an error in geolocation can also lead to over- or underestimating the height of the water pixels. It was seen that dark water pixels often resulted in bad height estimates, therefore this research concluded that it would be better to remove bad geolocation pixels and dark water pixels completely.

Another argument for avoiding 'dark water' pixels is that ice cover on lakes often is classified as dark water. Since the ice cover changes the backscattered signal, the water surface becomes more difficult to recognise, and is therefore categorised as dark water. When the backscattered signal is less strong, the height becomes more difficult to estimate, leading to increased WSE errors from dark water pixels. Fortunately, the dark water classification of ice-covered lakes works quite well, as can be seen from this example of a partially ice-covered lake. Therefore, by removing dark water pixels, most ice-covered pixels are also removed in this case. This results in a summer-bias in the yearly data record, because the summer period where the lake is ice-free contains more data and better consistency.

The naive approach to solve phase unwrapping errors showed that adding or subtracting an integer multiple of height to phase sensitivities could remove the slope in surface elevation, but for the case analysed here, this approach would result in a much lower surface elevation than what is measured by ICESat-2 because many phase ambiguities would have to be added. Furthermore, this approach is only valid for adding or subtracting a small number of phase ambiguities, but since this would not be enough to remove the surface slope of 20 m across the medium-sized lake, the better solution in this case is to recalculate the spatial unwrapping and phase unwrapping from scratch.

6.1.4. Limitations for Observing Small Lakes

Another important thing to mention is that the three chosen lakes have some of the best SWOT data records in their size category, because the lakes were chosen based on the available number of observations. Therefore, the resulting WSE error estimates are likely a lower boundary when considering all observed IMLs in Greenland. This is justified by the fact that only one year of observations were available and that it makes most sense to analyse the lakes which have the most observations to have enough data to draw significant conclusions. Lakes with fewer observations will eventually achieve more observations for future analysis. However, this bias was counteracted by choosing sample lakes of different sizes, such that the smallest lakes having the least amount of observations are still represented in the analysis.

Since SWOT has the goal of observing lakes as small as 1 ha (0.01 km^2) in area, it would have been best to include a lake of this size in the analysis as well, but this is not possible without a reference for the water surface elevation and gauged lakes are limited in Greenland. Since ICESat-2 only covers the ground beneath the narrow paths of the six beam tracks, smaller lakes may not be captured in the ICESat-2 observations if they lie between tracks. Finding such a small lake with reference data from ICESat-2 is challenging, which was already the case for finding the small lake included in this analysis. Additionally, the IML inventory of How et al. [24] only includes IMLs >0.05 km^2, which means that lakes smaller than 5 ha cannot be extracted from the SWOT data with this approach. Different sources than ICESat-2 could be used as reference for the mean WSE, such as a Digital Elevation Model (DEM) of Greenland. The problem with this approach would be that most sources (such as ArcticDEM) are at least a few years old, in which time IMLs can experience water level changes over several meters due to glacier melt or GLOF events. Thus, the water surface elevation in the DEMs will be outdated in many cases, making it impossible to distinguish whether the SWOT observations are wrong or the DEM is outdated if a discrepancy in water level is present.

Only very few lakes smaller than 1 km^2 were recognised in the SWOT data with more than 7 observations, which can partly be attributed to smaller lakes being observed less often, having fewer pixels, which leads to more observations being filtered out and being recognised less often as individual water bodies because they are missing in the PLD. This is part of the quality-quantity trade-off in obtaining SWOT observations, where choices have to be made between more data or better quality, such as with filtering out suspect geolocation quality pixels, setting a threshold for filtering out outliers based on STD and MAD and filtering out observations with too few pixels. According to Williams et al. [37], the geolocation and height show significant noise for land, dark water and low-coherence water, meaning that more accurate WSE estimates would be obtained if stricter filtering was applied. However, this would affect small lakes in particular, reducing their number of valid observations and thus excluding more small lakes from the observation records. On a global scale, the number of lakes increases with decreasing size. Thus, it is critical to include small lakes in the SWOT observations.

Initial results showed that SWOT-derived water surface elevations of ice marginal lakes are not accurate or consistent enough to find Glacial Lake Outburst Floods, which can happen from one observation to the next. For obtaining reliable storage changes from these data, it is necessary to look at longer time scales in the order of months or years, such as the change in water level which could be seen in the time series of lake Isortuarsuup Tasia.

6.2. Recommendations

6.2.1. Apply Strict Data Editing

This research has shown that strict data editing is required to obtain good quality WSE observations of ice marginal lakes in Greenland from the SWOT PIXC and LakeSP products. Based on this analysis, the most important data editing which should be applied to the PIXC product before retrieving WSE estimates are summarised below:

- Remove tidal components from PIXC height, as described in section 4.4 but do not use height-constrained geolocations because this will average the pixel heights.
- Remove land pixels, dark water and low coherence water with the classification parameter.
- Remove pixels with a bad geolocation, for which the value of the `geolocation_qual` variable is >28800 or even >4 to also remove suspect values.
- Restrict pixels to be included to reliable lake outlines from How et al.'s IML inventory or similar.
- Remove outliers with a difference to the following and previous point of more than 10 m (adjustable).
- After computing the STD and MAD of the height for all lake pixels of each observation, observations with a STD >20 m and MAD >10 m should be removed.

Some of the thresholds cannot be set objectively and have to be adjusted to the area of interest or the application for which the data is used. In this analysis, the threshold for the STD and MAD had to be adjusted for one lake individually, while the appropriate geolocation threshold was the same for all three lakes. It should also be considered to employ a time-dependent threshold. By setting a high threshold for the STD and MAD, more observations during the ice-covered periods will be obtained, but for the ice-free period a lower threshold is beneficial.

If a SWOT data user wishes to only use the LakeSP product and not the PIXC product for easier access, the following data editing should be applied to reduce the uncertainty of the WSE estimates depending on set thresholds:

- Remove lake features with an area larger than 131 km^2 (size of Romer Sø, the largest lake in Greenland).
- Use only lake observations intersecting Hows IML database or a similar database of IMLs.
- Use lakes which contain T or more observations, where the threshold T should be adjusted per application (in this study $T = 8$).
- Filter out outliers with a difference to the following and previous point of more than 10 m (also adjustable).
- Remove observations with a dark water fraction >85%.
- Remove observations with a WSE STD >2 m.
- Remove observations with a layover error >1 m.

Based on this filtering, the SWOT data should be validated against real-time gauge measurements if they are available.

Furthermore, the k-means clustering method can be used as a tool to find the high quality pixels of an observation, to provide a more accurate WSE estimate than the mean or median of all pixels without having to rely on the classification of pixels, but purely based on the coherence and σ_0. This method differs from simply filtering by classification or σ_0 alone, because it can combine the influence of multiple parameters simultaneously. In this way it is more robust to noisy pixels which by accident have a high σ_0 but not a high coherence or pixels which are wrongly classified as dark water.

6.2.2. Expand LakeSP Product

To be able to fully recreate the processing method of the LakeSP product and find solutions for improving the derived WSE, it is necessary to include additional variables which the WSE is based on, such

as the area and the outline over which the WSE is calculated. As a recommendation to the product managers, the `area_wse` and the geometry of this area should be included in the LakeSP product at least, to allow users a better understanding of the underlying data and provide a better possibility for error analysis.

Additionally, two changes to the LakeSP product should be taken into consideration. The first recommendation is to calculate the median WSE as well as the mean WSE for all lake observations, because this research showed how the mean can be influenced a lot more by individual pixels with erroneous height observations than the median. By implementing this small addition, users could choose the most fitting metric depending on the application, which would especially benefit challenging regions such as the Arctic or mountainous regions.

The second recommended change is to consider removing pixels classified as dark water and low coherence water entirely for calculating the LakeSP WSE, but this can have quite significant impacts on the number of available pixels, as has been discussed in chapter 4. An alternative would be to provide both a LakeSP product with dark water pixels and without dark water pixels, but since this would require large additional data storage, a more feasible approach is to use the `dark_frac` parameter to filter out observations with large percentages of dark water pixels. The difference is however that a product without dark water pixels can give good observations, even when the dark water fraction is high, while those observations will be filtered out when using the simpler approach.

In the end, inclusion of dark water pixels should always be based on an individual case-by-case evaluation. If the focus is on smaller lakes it may be necessary to keep them and resort to the other methods used here, but for larger lakes or for applications where less temporal resolution is needed, it is advised to remove them to reduce the uncertainty in water surface elevations.

Depending on the application, it should be decided whether a larger number of observations or a higher accuracy is favoured, such as to avoid error propagation. For large-scale hydrological modelling it can be more important that as many small lakes as possible are included to gain a better estimate of the total water storage. However, if the observation uncertainty is already in the order of 1 m or higher, the modelling becomes less accurate as well. To calculate storage changes or discharge, the accuracy can be more important than the number of observations because a decimeter difference in water level already has a large impact on the storage.

6.2.3. Improve the PLD

An extensive PLD provides the foundation for recognising and categorising lakes from the SWOT data. A detailed and accurate PLD is therefore essential for obtaining a good LakeSP product; however, this is not the case for Greenland. Initial investigation of IMLs in Greenland showed that several large lakes with documented GLOF behavior are missing from the PLD, such as lake Tordensø, lake Catalina and lake Iluliartoq. It has been documented that these lakes have experienced enormous storage changes, and it would therefore be especially beneficial to monitor their water level through SWOT observations. Furthermore, some IMLs are only partly present, such as lake Hullet shown in Figure 6.1. On the left side an optical image from Sentinel-2 is shown where the lake is partly covered by calving ice from the glacier front at the southern margin of the lake. This floating ice seems to cause a problem for the water detection in the PLD, because the right side shows the pixel cloud of the lake in blue, based on how it is present in the PLD. Notice that the missing part of the lake coincides quite well with the area covered by floating ice, where it is more difficult for SWOT to detect the underlying presence of water. This is especially an issue for ice marginal lakes, because they are often covered in calving ice from adjacent glaciers, making it more difficult to consistently detect the water surface. The floating ice can even persist in summer, when the rest of the lake surface is open water. An important recommendation is therefore to add ice marginal lakes present in other datasets to the PLD and thereby include more IML observations in the SWOT dataset.

6.2.4. Analyse Smaller Lakes

For continuous improvement and validation of the SWOT data it is highly recommended to analyse smaller lakes with areas of 1 ha or lower. These are still underrepresented in global validation efforts due to a lack of real-time reference data such as from gauges, and because fewer observations are available. Future research should determine how well these very small lakes are observed compared

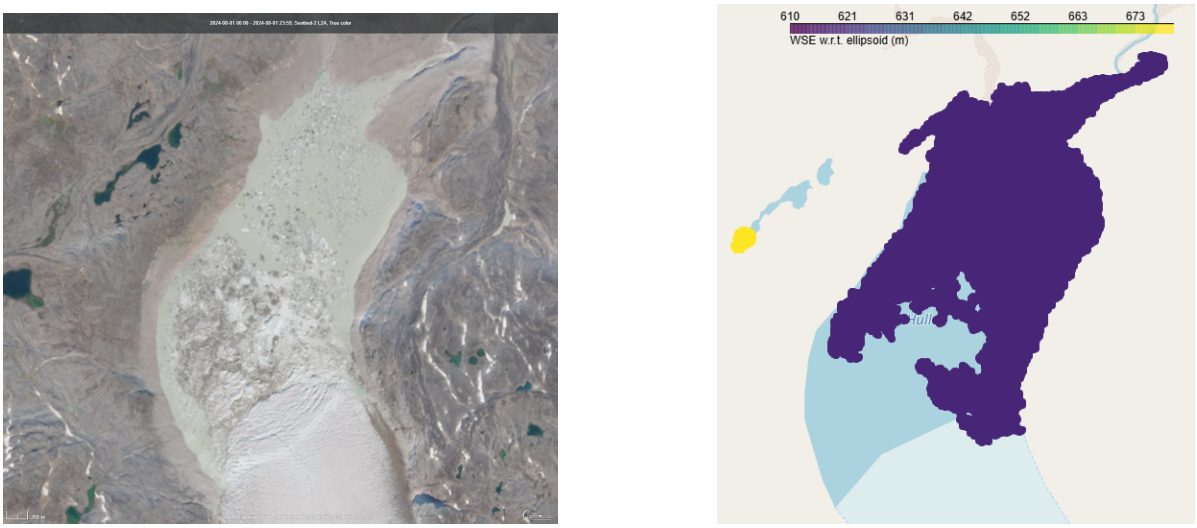

Figure 6.1: Lake Hullet as observed by Sentinel-2 (left) opposed to the pixel cloud from SWOT (right, in dark blue), which does not cover the lower part of the lake due to a wrong lake outline in the Prior Lake Database. The Sentinel-2 L2A true color image (01.08.2024) was downloaded via the Copernicus Browser [1].

to larger lakes, how small lakes can be observed consistently by SWOT and what role they play in global hydrology. This study aims to provide an initial step in answering these questions and should be regarded as a stepping stone, in particular, for using SWOT to observe lakes in challenging conditions and regions.

7

Conclusions

This research contributes to assess the performance of the Surface Water and Ocean Topography (SWOT) mission in observing the Water Surface Elevation (WSE) of lakes, with a focus on Ice Marginal Lakes (IMLs) in southwest Greenland as they are particularly challenging to observe.

Overall, SWOT has detected 535 IMLs in southwest Greenland, including small lakes which are often not covered by other altimeters such as ICESat-2, and provides an unprecedented frequency of lake elevation observations, even able to capture seasonal variation in the water surface elevation of lakes.

By comparing SWOT-derived WSEs from the Lake Single Pass Vector Product (LakeSP) and Pixel Cloud Data Product (PIXC) data products, it was found that the LakeSP product contains large data gaps when lakes are ice covered and experiences large WSE variability between observations. The PIXC product can be used to gain more good-quality observations during the ice covered periods by applying targeted filtering adapted to IMLs and employing the median WSE instead of the mean, which is more robust to outliers. However, PIXC is also computationally more expensive, while the LakeSP product is more efficient to analyse larger numbers of lakes or longer time periods. During the ice-free period, the LakeSP and PIXC products result in quite similar WSE estimates. For the three lakes analysed in this study, the WSEs show high consistency with ICESat-2 ATL06 height measurements. The WSE difference between SWOT observations and ICESat-2 (bias of 3.3 cm) for the three observed lakes are in the order of decimeters (0.27 - 1.38 m). Between SWOT observations a variability of 0.30 - 4.43 m was obtained depending on the lake and data product.

Before using either of these two SWOT data products to calculate the WSE, extensive data editing needs to be applied to reduce the WSE variability in order of several meters. In the PIXC product the large variability was already present between pixels in a single observation, while a large variability was present between observations in the LakeSP product. The main issues in the PIXC product are phase unwrapping errors, errors in the geolocation of pixels and ice cover leading to a low coherence and low Normalised Radar Cross-Section of the backscattered signal, characterised by dark water classification. Since the LakeSP product is a higher level product than the PIXC product, the aforementioned issues also affect the LakeSP product in addition to issues which are introduced in the processing. The main limitations for the LakeSP product are the specular ringing effects included in lake outline determination, insufficient assignment of lake ids, missing lakes and flawed outlines in the Prior Lake Database, and the influence of pixel outliers on the WSE determination.

Analyses of the WSE estimates from the LakeSP product and outliers from the PIXC product have shown that the WSE obtained from the LakeSP product can be improved through strict filtering based on the standard deviation, layover error and dark water fraction. However, it is not recommended to filter out observations based on the general quality flag or the ice cover flag because this would remove too many observations, including otherwise good observations.

To improve the PIXC product, bad geolocation quality, dark water and low coherence pixels should be filtered out because they often result in bad estimates of WSE. Additionally, single outliers and pixels

with a large STD or MAD (> 10 m) should be filtered out to reduce the large variability of WSE estimates.

A common problem for IMLs in Greenland seems to be a trade-off between quality and quantity of usable observations, therefore thresholds for data editing should be set depending on what the data are used for. The SWOT mission requirement for the WSE accuracy is not yet accomplished for IMLs in Greenland, but this research has shown that SWOT observations are under all circumstances providing far more frequent observations than ICESat-2 and are promising for observing more small lakes even under harsh conditions.

List of Figures

List of Tables

Bibliography

[1] Copernicus programme (Copernicus) and Copernicus Data Space Ecosystem. *Sentinel-2 L2A True color optical images, Copernicus Browser*. https://swot.jpl.nasa.gov/events/63/2024-swot-science-team-meeting/. Accessed: 2025-02-18. 2024.

[2] Jacob Bendle. *Glacial Lake Outburst Floods (GLOFs)*. https://www.antarcticglaciers.org/glaciers-and-climate/glacier-hazards/glacial-lake-outburst-floods/. Accessed: 2025-03-04. 2025.

[3] Sylvain Biancamaria, Dennis P Lettenmaier, and Tamlin M Pavelsky. "The SWOT mission and its capabilities for land hydrology". In: *Remote sensing and water resources*. Springer, 2016, pp. 117–147.

[4] David Boertmann et al. "The significance of SW Greenland as winter quarters for seabirds". In: *Bird Conservation International - BIRD CONSERV INT* 14 (June 2004). DOI: 10.1017/S0959270904000127.

[5] M. Brils, P. Munneke, and Michiel Van den Broeke. "Spatial Response of Greenland's Firn Layer to NAO Variability". In: *Journal of Geophysical Research: Earth Surface* 128 (Aug. 2023). DOI: 10.1029/2023JF007082.

[6] KM Brunt et al. "Comparisons of satellite and airborne altimetry with ground-based data from the interior of the Antarctic ice sheet". In: *Geophysical Research Letters* 48.2 (2021), e2020GL090572.

[7] Curtis Chen. *Surface Water and Ocean Topography (SWOT) Mission Science Team Meeting, Features of KaRIn Data that Users Should be Aware of*. 2024.

[8] Monica Coppo Frias et al. "River hydraulic modeling with ICESat-2 land and water surface elevation". In: *Hydrology and Earth System Sciences* 27.5 (Mar. 2023), pp. 1011–1032. DOI: 10.5194/hess-27-1011-2023.

[9] JPL D-109532. *SWOT Science Data Products User Handbook*. Tech. rep. Jet Propulsion Laboratory Internal Document, Pasadena, CA, 2024.

[10] Keren Dai et al. "Seasonal changes of glacier lakes in Tibetan Plateau revealed by multipolarization SAR data". In: *IEEE Geoscience and Remote Sensing Letters* 19 (2021), pp. 1–5.

[11] The Danish Agency for Data Supply and Infrastructure. *Satellitfoto Grønland*. https://dataforsyningen.dk/data/4783. Accessed: 2025-02-19. 2023.

[12] Francesco De Zan and A Monti Guarnieri. "TOPSAR: Terrain observation by progressive scans". In: *IEEE Transactions on Geoscience and Remote Sensing* 44.9 (2006), pp. 2352–2360.

[13] Paco López Dekkers. *AESM402B InSAR Part 1*. 2023.

[14] Mads Dømgaard et al. "Altimetry-based ice-marginal lake water level changes in Greenland". In: *Communications Earth & Environment* 5.1 (2024), p. 365.

[15] B. Du et al. "Synthesis Analysis of SWOT KaRIn-Derived Water Surface Heights and Local Cross-Calibration of the Baseline Roll Knowledge Error Over Lake Baikal". In: *Earth and Space Science* 8.11 (2021), e2021EA001990.

[16] Copernicus ESA and Sentiwiki. *Sentinel-3 Topography Mission Overview*. https://sentiwiki.copernicus.eu/web/s3-altimetry-instruments. Accessed: 2025-07-15.

[17] https://www.figma.com/board/xzh0zx2vEB73LqK7GG5IMA/Flowchart-LakeSP-timeseries?node-id=0-1&t=jhYm4qihZtaKqmg5-1. Accessed: 2025-06-02.

[18] Roger Fjørtoft, Nicolas Picot, and on behalf of the Cal/Val Team. *SWOT HR Lake Field Data Collection and SWOT Validation Meeting*. https://swot.jpl.nasa.gov/events/63/2024-swot-science-team-meeting/. Accessed: 2025-04-20. 2024.

[19] Roger Fjørtoft et al. “KaRIn-the Ka-band radar interferometer on SWOT: Measurement principle, processing and data specificities”. In: *IEEE International Geoscience and Remote Sensing Symposium*. IEEE. 2010, pp. 4823–4826.

[20] Roger Fjørtoft et al. “SWOT Hydrology Products and Early Results”. In: *IGARSS 2024-2024 IEEE International Geoscience and Remote Sensing Symposium*. IEEE. 2024, pp. 1410–1413.

[21] Lee-Lueng Fu et al. “The Surface Water and Ocean Topography Mission: A Breakthrough in Radar Remote Sensing of the Ocean and Land Surface Water”. In: *Geophysical Research Letters* 51.4 (2024). DOI: 10.1029/2023gl107652.

[22] Kartik/ GeeksforGeeks. *K means Clustering – Introduction*. https://www.geeksforgeeks.org/k-means-clustering-introduction/. Accessed: 2025-05-23.

[23] Ramon F Hanssen. *Radar interferometry: data interpretation and error analysis*. Vol. 2. Springer Science & Business Media, 2001.

[24] Penelope How et al. “Greenland-wide inventory of ice marginal lakes using a multi-method approach”. In: *Scientific Reports* 11.1 (2021), p. 4481.

[25] Louise Maubant, Lachlan Dodd, and Paul Tregoning. “Assessing the accuracy of SWOT measurements of water bodies in Australia”. In: *Geophysical Research Letters* 52.6 (2025), e2024GL114084.

[26] NASA NSIDC DAAC. *OpenAltimetry ICESat-2, EarthData*. https://openaltimetry.earthdatacloud.nasa.gov/data/icesat2/. Accessed: 2025-04-10.

[27] Girish Patidar, J Indu, and Subhankar Karmakar. “Performance assessment of Surface Water and Ocean Topography (SWOT) mission for WSE measurement across India”. In: *Geophysical Research Letters* 52.10 (2025), e2025GL115804.

[28] A. Dassel/ Pixabay and ESA. *Prince Christian Sound, Greenland*. https://www.esa.int/Applications/Observing_the_Earth/FutureEO/CryoSat/Ice_loss_from_Greenland_and_Antarctica_hits_new_record. Accessed: 2025-05-20.

[29] Claire Pottier, Roger Fjørtoft, and on behalf of the HR Cal/Val Team. *SWOT HR Lake Product Validation*. Tech. rep. Accessed: 2025-04-20. Centre National d’Etudes Spatiales (CNES), 2024.

[30] Claire Pottier and Cassie Stuurman. *SWOT Product Description Document: Level 2 KaRIn High Rate Lake Single Pass Vector Product (L2_HR_SP)*. Tech. rep. Revision C (Draft). Centre National d’Etudes Spatiales, 2024.

[31] Kristina P Sinaga and Miin-Shen Yang. “Unsupervised K-means clustering algorithm”. In: *IEEE access* 8 (2020), pp. 80716–80727.

[32] B. Smith et al. *ATLAS/ICESat-2 L3A Land Ice Height, Version 6, User Guide*. Tech. rep. Accessed: 2025-04-23. NASA National Snow et al., 2023.

[33] B. Smith et al. *Ice, Cloud, and Land Elevation Satellite (ICESat-2) Project Algorithm Theoretical Basis Document (ATBD) for Land Ice Along-Track Height Product (ATL06), Version 6*. Tech. rep. ICESat-2 Project, 2022. DOI: 10.5067/VWOKQDYJ7ODB.

[34] Muhammad Ali Syakur et al. “Integration k-means clustering method and elbow method for identification of the best customer profile cluster”. In: *IOP conference series: materials science and engineering*. Vol. 336. IOP Publishing. 2018, p. 012017.

[35] Jida Wang et al. *SWOT’s capabilities and early science results for global lakes and reservoirs*. https://swot.jpl.nasa.gov/events/63/2024-swot-science-team-meeting/. Accessed: 2025-04-20. 2024.

[36] Jida Wang et al. “The Surface Water and Ocean Topography Mission (SWOT) Prior Lake Database (PLD): Lake Mask and Operational Auxiliaries”. In: *Water Resources Research* 61.3 (2025), e2023WR036896.

[37] Brent Williams. *Surface Water and Ocean Topography (SWOT) Mission, PIXC Validation*. https://swot.jpl.nasa.gov/events/63/2024-swot-science-team-meeting/. Accessed: 2025-04-20. 2024.

[38] Brent Williams. *SWOT PIXC Dataset Phase Unwrapping on a local machine*. https://podaac.github.io/tutorials/notebooks/datasets/SWOT_PIXC_PhaseUnwrap_localmachine.html. Accessed: 2025-02-19. 2023.

[39] Zhaonan Xue, Lin Liu, and Houjun Jiang. “Detection of effective imaging area of SWOT satellite in the Xizang Plateau”. In: *Geodesy and Geodynamics* 16.2 (2025), pp. 203–213.

[40] Wei Yan et al. “Outburst flood forecasting by monitoring glacier-dammed lake using satellite images of Karakoram Mountains, China”. In: *Quaternary International* 453 (2017), pp. 24–36.

[41] Fangfang Yao et al. “Leveraging ICESat, ICESat-2, and landsat for global-scale, multi-decadal reconstruction of lake water levels”. In: *Water Resources Research* 60.2 (2024), e2023WR035721.

[42] Ding Yongjian and Liu Jingshi. “Glacier lake outburst flood disasters in China”. In: *Annals of Glaciology* 16 (1992), pp. 180–184.

A

Appendix

A.1. Introduction to k-means Clustering

k-means clustering is a common machine learning algorithm useful to group data into k number of clusters based on similarity [34]. The algorithm requires the number of clusters k to be specified and initial centroid points of the clusters to be set, either from estimates or at random. If $\mathbf{X} = \{x_1, ..x_n\}$ is our data set in d dimensions, and $\mathbf{A} = \{a_1, ..a_k\}$ are the cluster centroids up to k clusters, the objective function to minimise is [31]:

$$J(z, A) = \sum_{i=1}^{n} \sum_{c=1}^{k} z_{ic} ||x_i - a_c||^2 \tag{A.1}$$

Here, $||x_i - a_c||^2$ is the euclidean distance between each data point x_i and each cluster centroid a_c and z_{ic} is a $n \times k$ matrix of binary variable describing which cluster each data point is assigned to:

$$z_{ic} = \begin{cases} 1, & \text{if } ||x_i - a_c||^2 = \min_{1 \le c \le k} ||x_i - a_c||^2 \\ 0, & \text{otherwise} \end{cases} \tag{A.2}$$

Thus, each d-dimensional data point x_i is assigned to the cluster which has the smallest euclidean distance to its centroid a_c.

From all points belonging to a cluster, a new centroid is found, minimizing the within cluster sum of squares (WCSS) or variance:

$$a_c = \frac{\sum_{i=1}^{n} z_{ic} x_{ij}}{\sum_{i=1}^{n} z_{ic}} \tag{A.3}$$

Essentially, this sums up all values of points belonging to the cluster (for which $z_{ic} = 1$) and divides by the number of points in the cluster to find the cluster centroid in each dimension. Based on these new centroids, the euclidean distances of each point to each centroid is calculated again and assigned to the cluster with minimum distance. This process is repeated until the centroids no longer change significantly or a maximum number of iterations has been reached, thus minimising the objective function and the WCSS. In Figure A.1 it is illustrated how the clustering would look in 2D, but the analysis performed in this study contains many dimensions.

A.2. Additional Figures

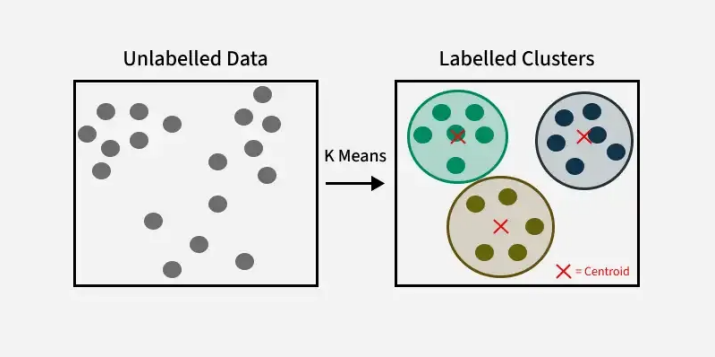

Figure A.1: Basic Example of k-means clustering in 2D [22].

	Bit (from LSB)	Decimal	geolocation_qual
	0	1	layover_significant
	1	2	phase_noise_suspect
Suspect	2	4	phase_unwrapping_suspect
	3	8	model_dry_tropo_cor_suspect
	4	16	model_wet_tropo_cor_suspect
	5	32	iono_cor_gim_ka_suspect
	6	64	xovercal_suspect
	7	128	
	8	256	
	9	512	
	10	1024	
	11	2048	
	12	4096	medium_phase_suspect
	13	8192	tvp_suspect
	14	16384	sc_event_suspect
	15	32768	small_karin_gap
Degraded	16	65536	
	17	131072	
	18	262144	
	19	524288	specular_ringing_degraded
	20	1048576	model_dry_tropo_cor_missing
	21	2097152	model_wet_tropo_cor_missing
	22	4194304	iono_cor_gim_ka_missing
	23	8388608	xovercal_missing
	24	16777216	geolocation_is_from_refloc
Bad	25	33554432	
	26	67108864	
	27	134217728	no_geolocation_bad
	28	268435456	medium_phase_bad
	29	536870912	tvp_bad
	30	1073741824	sc_event_bad
	31	2147483648	large_karin_gap

Ignore these bits

Figure A.2: Bitwise geolocation quality flag showing all declared issues and their corresponding bitwise and decimal value, from the less severe to the more severe issues.

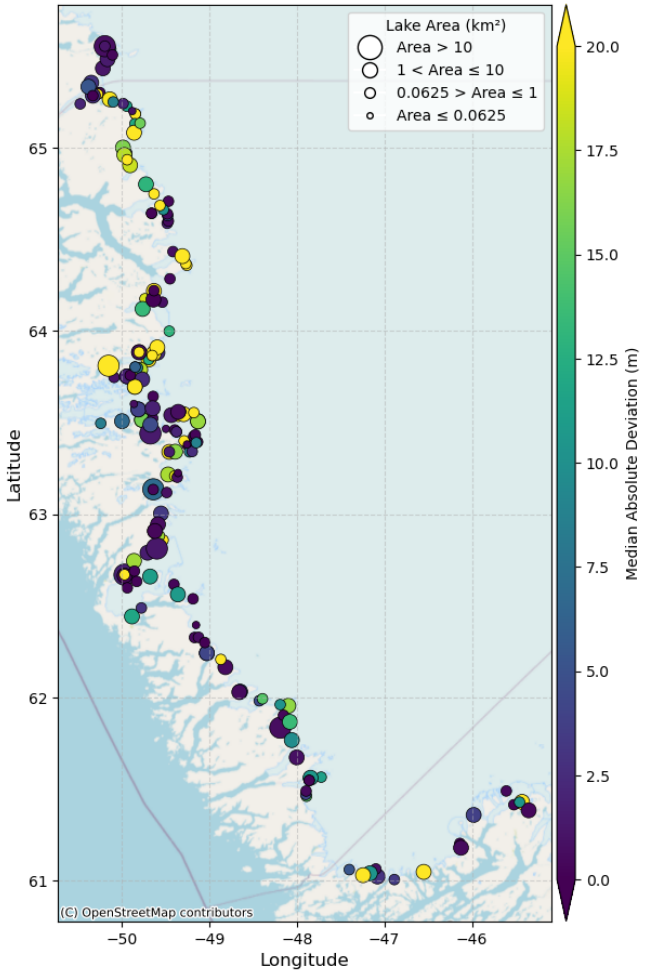

Figure A.3: Map of SWOT-observed IMLs in southwest Greenland coloured according to the magnitude of the MAD over all observations of that lake in time.

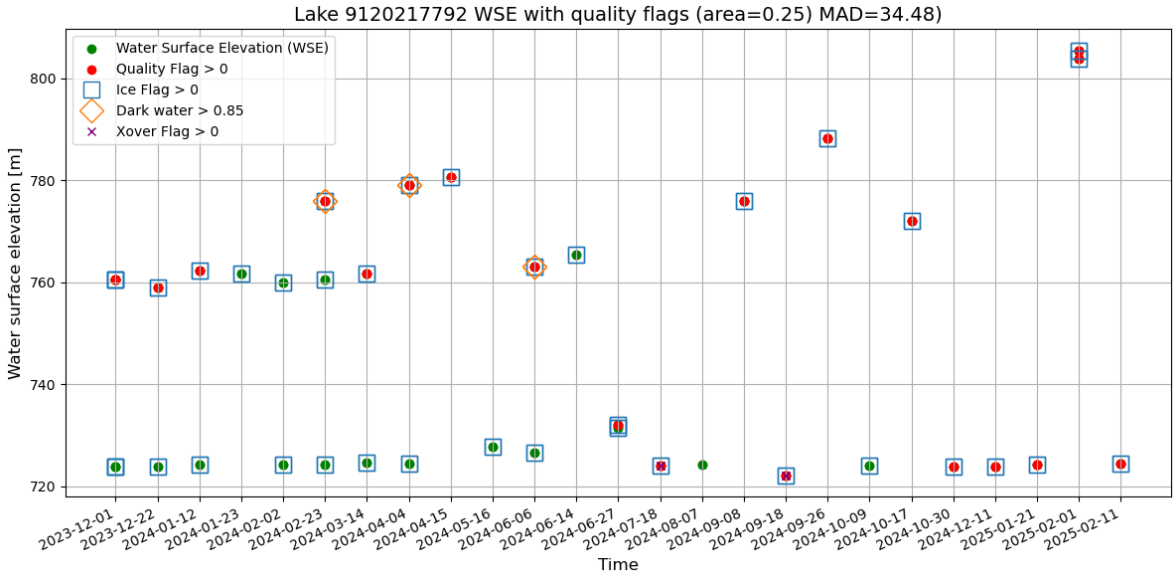

Figure A.4: Time series of all observations assigned to one lake id with suspiciously many observations and high MAD. From the two horizontal lines of observations it can be suspected that two lakes are observed instead of one.

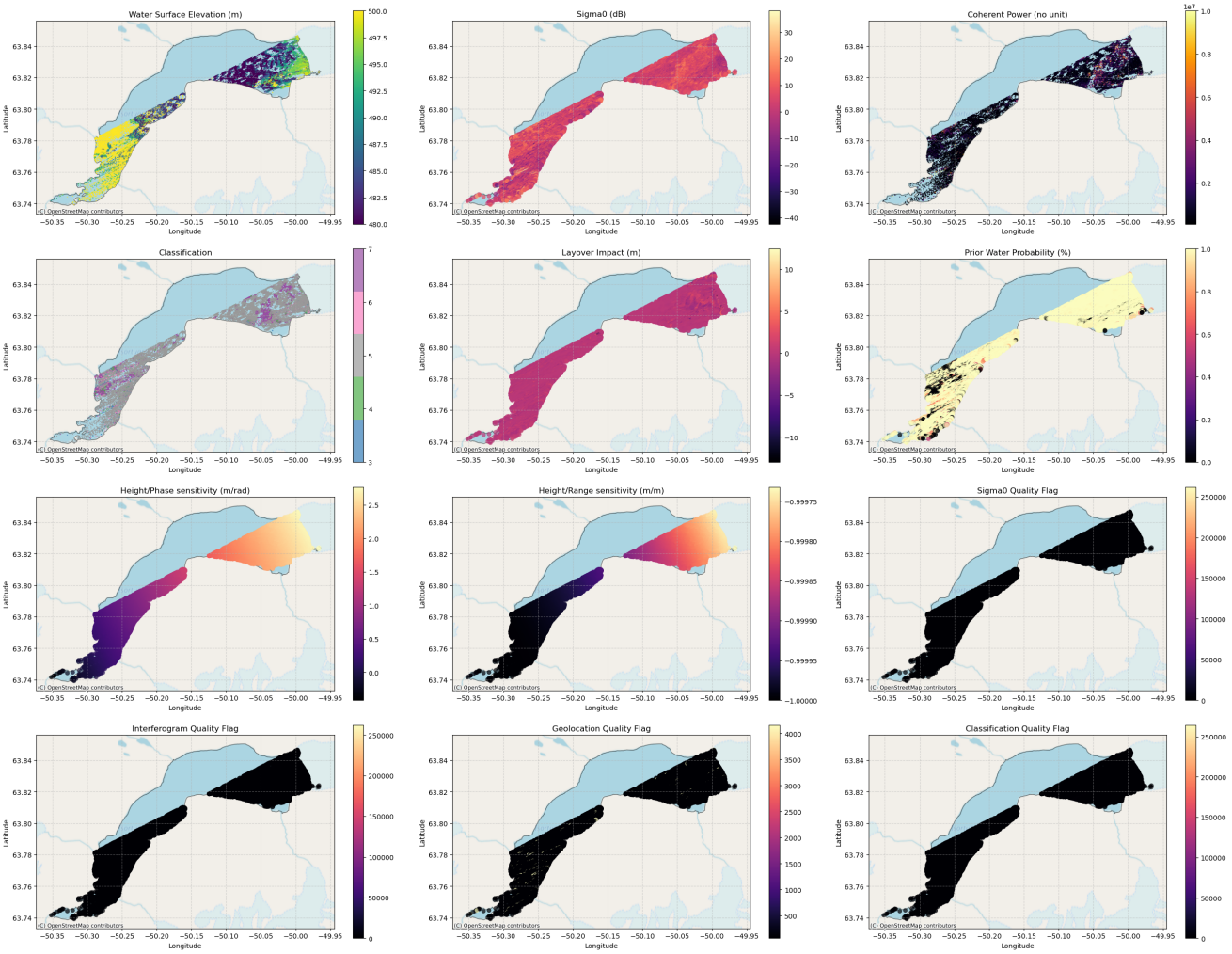

Figure A.5: Observation of the lake Isortuarsuup Tasia on 17.09.2024 with maps of the height, and relevant parameters from the PIXC product.

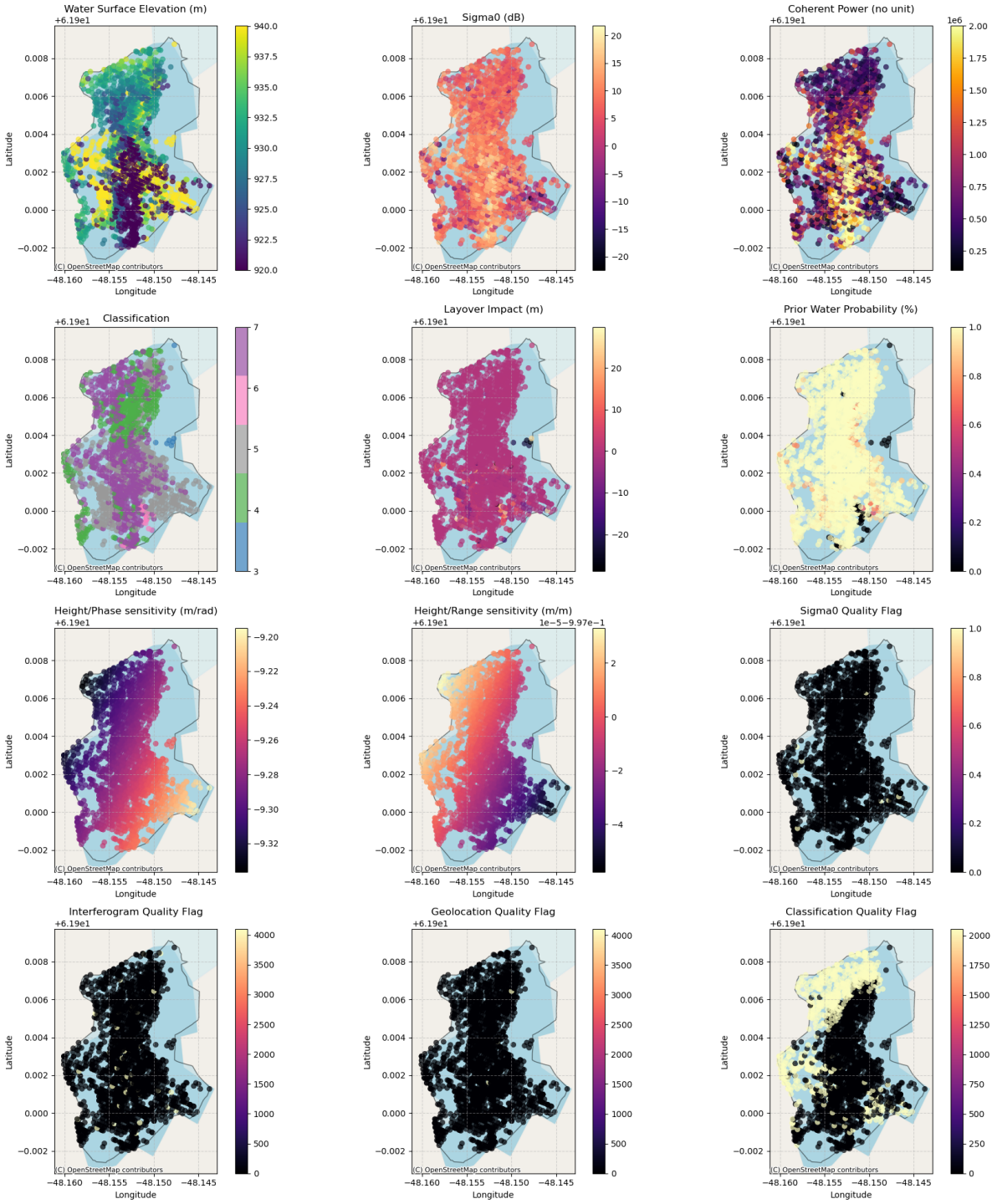

Figure A.6: Observation of the small lake on 21.02.2024 with maps of the height, and relevant parameters from the PIXC product.

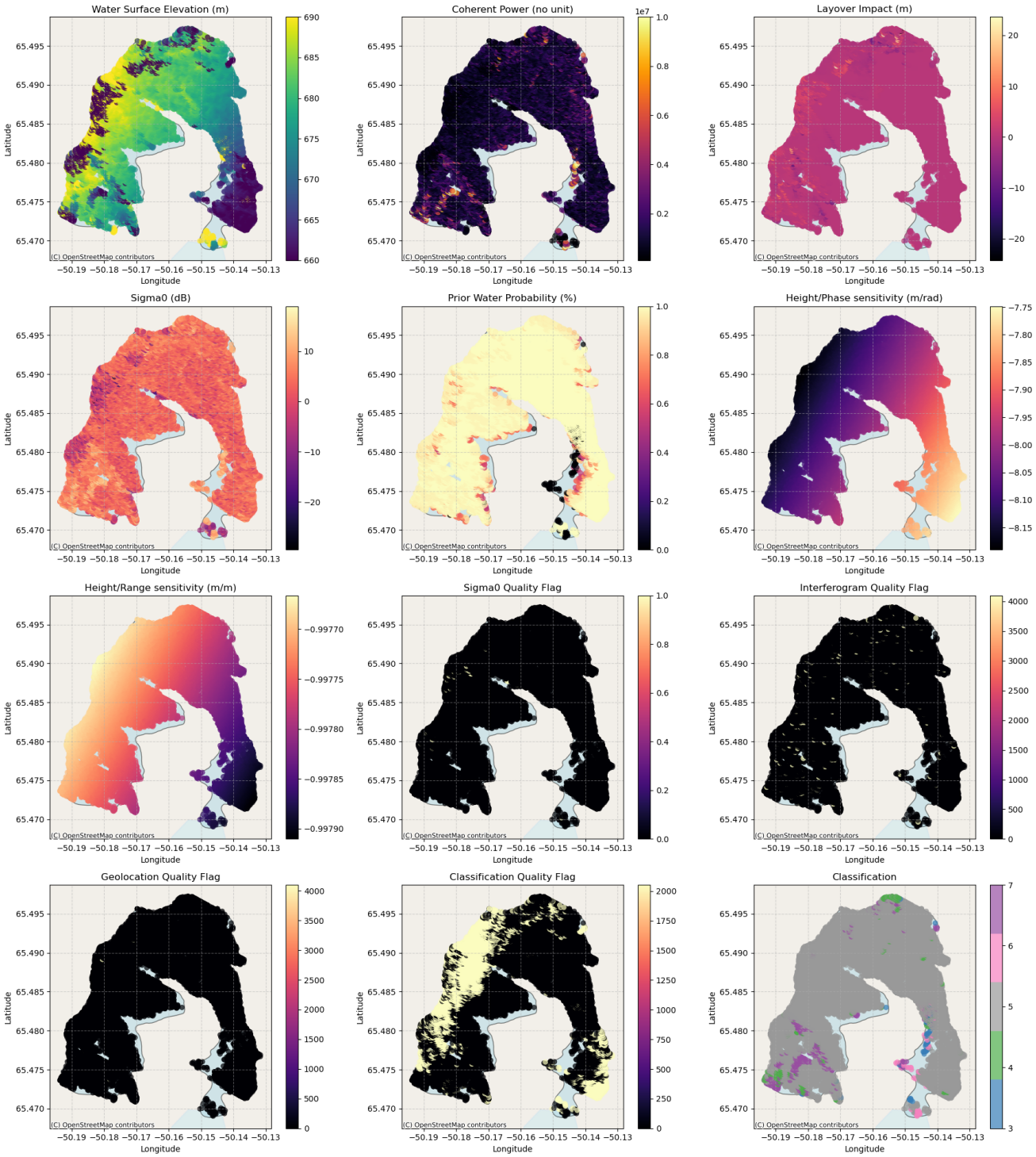

Figure A.7: Observation of the medium-sized lake on 13.02.2024 with maps of the height, and relevant parameters from the PIXC product. The WSE shows a strong gradient over the lake, thus resulting in a bad WSE estimate.